

---

# When and How to Canonize: A Generalization Perspective

---

**Yonatan Sverdlov\***

Technion – Israel Institute of Technology

**Benjamin Friedman**

Technion – Israel Institute of Technology

**Snir Hordan**

Technion – Israel Institute of Technology

**Nadav Dym**

Technion – Israel Institute of Technology

## Abstract

While invariant architectures are standard for processing symmetric data, there is growing interest in achieving invariance by applying group averaging or canonization to non-invariant backbones. However, the theoretical generalization properties of these alternative strategies remain poorly understood. We introduce a theoretical framework to analyze the generalization error of these methods by bounding their covering numbers. We establish a rigorous generalization hierarchy: the error bounds of canonized models are at best equal to the error bounds of structurally invariant and group-averaged models, and at worst equal to the bounds of non-invariant baselines. Furthermore, we show that there exist “optimal” canonizations which attain the optimal error bounds, and “poor” canonizations which attain the non-invariant error bounds, and that this depends on the regularity of the canonization. Finally, applying this framework to permutation groups in point cloud processing, we rigorously prove that the covering number of lexicographical sorting grows exponentially with point cloud dimension, whereas Hilbert curve canonization guarantees polynomial growth. This provides the first formal theoretical justification for the empirical success of Hilbert curve serialization in state-of-the-art point cloud architectures. We conclude with experiments that support our theoretical claims.

Our Code is available at <https://github.com/yonatansverdlov/Canonization>

## 1 Introduction

The integration of geometric priors into neural networks has become a cornerstone of modern machine learning, particularly for applications involving graphs, 3D point clouds, and molecular structures. In these domains, the underlying data often exhibits inherent symmetries, meaning the target function to be learned is invariant to a specific group action. Exploiting these symmetries is known to improve sample complexity and generalization [8, 5].

While specialized architectures, which are invariant by design, are a common method for processing symmetric data, there is growing interest in achieving invariance by applying generalized group averaging methods to non-invariant backbones. This family of methods includes full group averaging, which is theoretically sound but intractable for all but very small groups, group augmentation, which can be seen as an efficient approximation of group averaging, frame averaging [23], which enables invariant averaging over subsets of the group, and canonization, which maps every group orbit to a single, consistent “canonical” element.

---

\*Corresponding author, Emails: [yonatans@campus.technion.ac.il](mailto:yonatans@campus.technion.ac.il), [benjamin.fri@campus.technion.ac.il](mailto:benjamin.fri@campus.technion.ac.il), [snirhordan@campus.technion.ac.il](mailto:snirhordan@campus.technion.ac.il), [nadavdym@technion.ac.il](mailto:nadavdym@technion.ac.il).

Canonization is the most efficient of all generalized group averaging methods, as it only involves processing a single orbit representative. At the same time, it enjoys the same universal approximation guarantees as full group averaging [14]. These observations have motivated researchers to define canonizations in several diverse domains. These include sign canonizations for spectral embeddings of graphs [20, 18, 12], canonizations of graphs [17] and point clouds [14, 2, 10, 34] including the celebrated Point Transformer V3 [30], and canonization of the SMILES representation of small molecules [29].

In this paper, we provide a theoretical study of canonization from the perspective of generalization. Our focus is both on comparing canonization with other options for enforcing invariance and on comparing the quality of different canonizations. Our main contributions are threefold:

1. **Canonization vs. Group Averaging:** We prove that the generalization bounds of canonized models are at best equal to the bounds of group-averaged models, and at worst equal to the bounds of non-invariant models (Section 2).
2. **Canonizations and continuity:** We show that continuous, isometric canonizations attain the *optimal* generalization error achieved by group averaging, while discontinuous canonizations can lead to *poor* canonizations whose error bounds are identical to non-invariant models (Section 3).
3. **Hilbert Canonization:** We prove that canonizing point clouds with respect to permutation via lexicographical sorting is inferior to the Hilbert canonizations used in Point Transformer V3 [30], thus establishing the first theoretical justification for the empirical success of this method (Section 4).

## 1.1 Related Work

**Canonization vs. Group Averaging** It was observed that randomized SMILES can often outperform canonized SMILES [1, 3] (see also [13]). Our first contribution gives a theoretical justification for this empirical observation.

**Discontinuity** It was shown in [7, 2] that in many invariant learning scenarios, continuous canonizations are mathematically impossible. Attempts to mitigate this issue were made in [27, 16]. Our second contribution complements these works by showing how discontinuity of canonization hurts the generalization of the canonized model.

**Invariance and Generalization** Many papers have considered generalization analysis of invariant models [28, 22, 21, 9], but they do not consider canonizations. To our knowledge, the only paper considering the generalization of canonizations is [26]. They prove that in some setting the *approximation error* of canonized models is lower than group averaged models, and as a result the *expected error* of canonized models can be lower when the model is presented with enough samples. In contrast, our first conclusion is that the *generalization error bound* of group average models is always lower than the generalization error bound of canonized models.

## 1.2 Notation

Throughout the paper, we will consider a metric space  $(K, \rho)$ , where  $K$  is endowed by the action of a group  $\mathbb{G}$ . We will assume that the metric is  $\mathbb{G}$  invariant, i.e.,  $\rho(g \cdot x, g \cdot y) = \rho(x, y)$  for all  $x, y \in K$  and  $g \in \mathbb{G}$ .

**Quotient space** We denote the orbit of  $x \in K$  by  $[x] = \{g \cdot x \mid g \in G\}$ , and denote the quotient space to be the space of orbits  $K/\mathbb{G} := \{[x] \mid x \in K\}$ . On this space, we define a metric  $\rho_{\mathbb{G}}([x], [y]) := \min_{g \in \mathbb{G}} \rho(g \cdot x, y)$ , where we explicitly assume that the minimum in the definition of  $\rho_{\mathbb{G}}$  exists, which is the case in most examples of practical interest. This assumption, together with the  $\mathbb{G}$  invariance of  $\rho$ , guarantees that  $\rho_{\mathbb{G}}$  is a metric. We call a triplet  $(K, \rho, \mathbb{G})$  satisfying the conditions of the last two paragraphs a *module*.

**Covering number** Let  $(K, \rho)$  be a metric space. We say that  $C \subset K$  is an  $\epsilon$  cover of  $K$ , if  $\forall x \in K, \exists y \in C : \rho(x, y) \leq \epsilon$ . The minimal  $N$  such that there exists an  $\epsilon$  cover of cardinality  $N$  is called the  $\epsilon$  covering number of  $K$ , and is denoted by  $\mathcal{N}(K, \rho, \epsilon)$ .

**Canonization** We say that  $c : K \rightarrow K$  is a canonization if for every  $x \in K$ , (i)  $c(x) \in [x]$ , and (ii) all  $y \in [x]$  satisfy  $c(y) = c(x)$ . We will sometimes use *canon.* as an abbreviation for canonization.

## 2 Generalization, Canonization and Group Averaging

Our discussion of the generalization properties of canonizations and other invariant models is based on a popular framework from [32] for studying generalization via metric properties like Lipschitz continuity and covering numbers. We begin with a short review of this framework.

Consider a supervised learning problem of learning an unknown function  $f : X \rightarrow Y$  from a finite set of  $n$  samples  $S = \{(x_i, f(x_i)) \mid i = 1, \dots, n\}$  of the function. Assume that we have some algorithm (e.g., gradient descent) which, given  $S$ , returns a hypothesis  $h_S : X \rightarrow Y$ . Let  $\ell : Y \times Y \rightarrow \mathbb{R}$  be a function which will be used as a loss function. The *expected loss*  $\mathcal{L}$  and the *empirical loss*  $\mathcal{L}_{\text{emp}}$  are defined via

$$\mathcal{L}_{\text{exp}}(h_S) \triangleq \mathbb{E}_{x \sim \mu} \ell(h_S(x), f(x)), \quad \mathcal{L}_{\text{emp}}(h_S) \triangleq \frac{1}{n} \sum_{i=1}^n \ell(h_S(x_i), f(x_i))$$

The *generalization error* measures how much the empirical error of  $h_S$  on the training data can deviate from its true loss (the expected loss) on the data distribution. It can be bounded using the Lipschitz constants of the function  $h_S, f, \ell$  and the covering number of the domain  $X$ , as follows:

**Theorem 2.1.** [Proof in Appendix A.1, based on [32]] Let  $(X, \rho)$  and  $(Y, \rho_Y)$  be metric spaces and assume  $X$  is compact. Let  $f : X \rightarrow Y$  be a  $c_f$  Lipschitz function, and let  $\ell : Y \times Y \rightarrow [0, M]$  be a  $c_\ell$  Lipschitz function. Then for any  $\epsilon, \delta > 0$  and natural  $n$ , for a training sample set  $S$  generated by  $n$  IID draws from a distribution  $\mu$ , with probability of at least  $1 - \delta$ , we have

$$|\mathcal{L}_{\text{exp}}(h_S) - \mathcal{L}_{\text{emp}}(h_S)| \leq 2c_\ell(c_{h_S} + c_f)\epsilon + M \sqrt{\frac{2\mathcal{N}(X, \rho, \epsilon) \ln 2 + 2 \ln(1/\delta)}{n}}$$

where  $c_{h_S}$  denotes the Lipschitz constant of  $h_S$ .

We now apply this theorem in the setting where the learned function  $f$  is invariant to a group action. Our focus is on the setting where we have a non-invariant Lipschitz backbone  $\tilde{h}$ , and we consider three types of models: (i) models that do not incorporate symmetry  $h = \tilde{h}$ , (ii) models that incorporate symmetries by canonization,  $h = \tilde{h} \circ c$  and (iii) models that incorporate symmetries by group averaging  $h(x) = \int_G \tilde{h}(gx) dg$ . In this setting, the averaged function  $h$  is invariant and has the same Lipschitz constant as  $\tilde{h}$  (see Proposition A.2 in the appendix). Our proposition below will be relevant for any Lipschitz invariant model, whether obtained via averaging or via a specialized invariant model:

**Proposition 2.2.** [Proof in Appendix A.1] Let  $(K, \rho, \mathbb{G})$  be a module. Let  $(Y, \rho_Y)$  be a metric space, and assume  $K$  is compact. Let  $f : K \rightarrow Y$  be a  $c_f$  Lipschitz function **which is  $\mathbb{G}$  invariant**, and let  $\ell : Y \times Y \rightarrow [0, M]$  be a  $c_\ell$  Lipschitz function, then for any  $\epsilon, \delta > 0$  and natural  $n$ , for a training sample set  $S$  generated by  $n$  IID draws from the distribution  $\mu$ , with probability of at least  $1 - \delta$ , we have

$$|\mathcal{L}_{\text{exp}}(h_S) - \mathcal{L}_{\text{emp}}(h_S)| \leq 2c_\ell(c_{h_S} + c_f)\epsilon + M \sqrt{\frac{2\mathcal{N}(h_S) \ln 2 + 2 \ln(1/\delta)}{n}}$$

where

$$\mathcal{N}(h_S) = \begin{cases} \mathcal{N}(K, \rho, \epsilon) & \text{if } h_S \text{ is } c_{h_S} \text{ Lipschitz} \\ \mathcal{N}(c(K), \rho, \epsilon) & \text{if } h_S = \tilde{h}_S \circ c, \tilde{h}_S \text{ is } c_{h_S} \text{ Lipschitz, and } c \text{ is a canon.} \\ \mathcal{N}(K/\mathbb{G}, \rho_{\mathbb{G}}, \epsilon) & \text{if } h_S \text{ is } c_{h_S} \text{ Lipschitz and } \mathbb{G} \text{ invariant} \end{cases} \quad (1)$$

*Proof idea.* The claim for a Lipschitz function  $h_S$  without any invariant structure follows immediately from Theorem 2.1. For a function of the form  $h_S = \tilde{h}_S \circ c$ , the claim follows from Theorem 2.1 when replacing the domain  $K$  with  $c(K)$  and the function  $h_S$  with  $\tilde{h}_S$ . The claim for  $h_S$  which is both Lipschitz and invariant follows from the fact that due to invariance  $h_S, f$  can be identified with function  $\hat{h}_S, \hat{f} : K/\mathbb{G} \rightarrow Y$  satisfying  $\hat{h}_S([x]) = h_S(x), \hat{f}([x]) = f(x), \forall x \in K$ , and the Lipschitz constant remains unchanged after the identification (see Lemma 20 in [24]).  $\square$

For each of the three model types considered in Proposition 2.2, a different value of  $\mathcal{N}(h_S)$  is provided. The following simple lemma establishes the relationship between these three values:

**Proposition 2.3.** *For any module  $(K, \rho, \mathbb{G})$ , and any  $\epsilon > 0$ , the following inequality holds:*

$$\mathcal{N}(K/\mathbb{G}, \rho_{\mathbb{G}}, \epsilon) \leq \mathcal{N}(c(K), \rho, \epsilon) \leq \mathcal{N}(K, \rho, \epsilon) \quad (2)$$

*Proof.* The inequality  $\mathcal{N}(c(K), \rho, \epsilon) \leq \mathcal{N}(K, \rho, \epsilon)$  is immediate since  $c(K) \subseteq K$ . The inequality  $\mathcal{N}(K/\mathbb{G}, \rho_{\mathbb{G}}, \epsilon) \leq \mathcal{N}(c(K), \rho, \epsilon)$  is due to the quotient mapping  $q(x) = [x]$  being onto and 1-Lipschitz, and therefore it transforms any  $\epsilon$  cover of  $c(K)$  to an  $\epsilon$  cover of  $K/\mathbb{G}$ .  $\square$

Proposition 2.2 and Proposition 2.3 lead to the following conclusion:

### Conclusion 1

The generalization bounds of canonized models are at best equal to the bounds of group-averaged models, and at worst equal to the bounds of non-invariant models.

In Section 5 we give empirical support for this claim, by providing several experiments in which group averaging outperforms canonized models. At the same time, we note that group averaging requires more computational resources and is infeasible for large groups. Thus, Conclusion 1 implies that the improved complexity of the canonized model comes at the price of reduced generalization, but it is not a conclusive statement that canonization should be avoided.

We conclude this section by showing that the ratio between the largest and smallest covering numbers in (2) is bounded by the group's cardinality, implying that for larger groups the gap between non-invariant, canonized, and averaged models will be more pronounced:

**Proposition 2.4.** *[See proof in A.2] Let  $(K, \rho, \mathbb{G})$  be a module, and assume  $\mathbb{G}$  is finite. Then*

$$\mathcal{N}(K, \rho, \epsilon) \leq |\mathbb{G}| \cdot \mathcal{N}(K/\mathbb{G}, \rho_{\mathbb{G}}, \epsilon).$$

## 3 Canonizations and Continuity

In the previous section, we established upper and lower bounds for the covering numbers of canonizations. Our focus in this section is to study when these bounds are achieved.

**Definition 3.1.** Let  $(K, \rho, \mathbb{G})$  be a module and let  $\epsilon$  be a positive number. We say that  $c$  is  $(K, \epsilon)$  *optimal* if it attains the lower bound in (2), namely  $\mathcal{N}(c(K), \rho, \epsilon) = \mathcal{N}(K/\mathbb{G}, \rho_{\mathbb{G}}, \epsilon)$ . We say that  $c$  is  $(K, \epsilon)$  *poor* if it attains the upper bound in (2), namely  $\mathcal{N}(c(K), \rho, \epsilon) = \mathcal{N}(K, \rho, \epsilon)$ .

We will next show conditions for optimal and poor canonizations, and show how these conditions relate to the continuity of the canonization.

**Optimal canonizations:** First, we prove that canonizations, which are isometries, are optimal. We say that a canonization  $c : K \rightarrow K$  is an *isometry* if  $\rho(c(x), c(y)) = \rho_{\mathbb{G}}([x], [y])$  for all  $x, y \in K$ .

**Proposition 3.2.** *[proof in A.2] Any isometric canonization  $c : K \rightarrow K$  is  $(K, \epsilon)$  optimal for all  $\epsilon > 0$ .*

We next use this claim to give several examples of optimal canonizations:

**Example 3.3.** The following canonizations are isometries (see proof in A.2)

1. The canon.  $c(x) = |x|$  with respect to the action of  $\{-1, 1\}$  on  $\mathbb{R}$  and the standard metric.
2. The canon.  $\text{sort} : \mathbb{R}^n \rightarrow \mathbb{R}^n$  with respect to the action of permutations and a metric  $\rho$  induced by a  $p$  norm.
3. The centralization canon. defined for point clouds in  $\mathbb{R}^{d \times n}$  with respect to the action of translation by vectors in  $\mathbb{R}^d$ , with the metric  $\rho$  induced by the Frobenius norm.

In Proposition A.3 in the appendix, we prove that a canonization is isometric if and only if it is 1-Lipschitz in the standard sense. In particular, this means that an isometric canonization is always continuous. As a result, in the setting where there can be no continuous canonizations, such as

those discussed in [7, 2], there can be no isometric canonizations. **Poor canonizations:** We next show that discontinuities in canonizations can lead to poor canonizations. This occurs under two conditions: firstly, the canonization is ‘strongly discontinuous’ in the sense that it has  $|G|$  partial limits. Secondly, the domain  $K$  of the group action is chosen adversarially to exploit the discontinuity of the canonization.

**Proposition 3.4.** [proof in A.2] Let  $(V, \rho, \mathbb{G})$  be a module, where  $\mathbb{G}$  is a finite group. Let  $c$  be a canonization that has  $|G|$  partial limits at a point  $x \in V$ . Then for any small enough  $\epsilon > 0$  there exists a  $\mathbb{G}$  invariant set  $K \subseteq V$  such that  $\mathcal{N}(c(K), \rho, \epsilon) = \mathcal{N}(K, \rho, \epsilon) = |\mathbb{G}| \cdot \mathcal{N}(K/\mathbb{G}, \rho, \epsilon)$ .

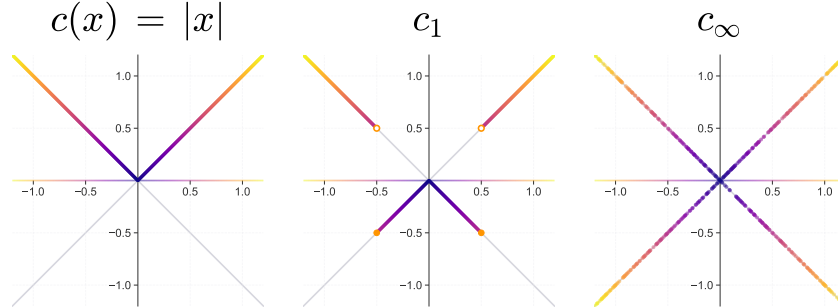
Based on this proposition, we give two examples of poor canonizations:

**Example 3.5.** Consider the action of  $\mathbb{G} = \{-1, 1\}$  on  $\mathbb{R}$ . Consider the canonizations

$$c_1(t) = \begin{cases} |t| & \text{if } |t| > 1/2 \\ -|t| & \text{if } |t| \leq 1/2 \end{cases}, \quad c_\infty(t) = \begin{cases} |t| & \text{if } t \in \mathbb{Q} \\ -|t| & \text{if } t \notin \mathbb{Q} \end{cases}$$

visualized in Figure 1. Both of these canonizations are discontinuous and have a point with  $|G| = 2$  partial limits. Therefore, by Proposition 3.4 for every small enough  $\epsilon > 0$  we can choose an adversarial domain for which the canonization is poor. For  $c_1$  we can choose for every  $\epsilon \in (0, 1)$  the set  $K = B_\epsilon(-\frac{1}{2}) \cup B_\epsilon(\frac{1}{2})$  and then  $\mathcal{N}(K, \rho, \epsilon) = \mathcal{N}(c_1(K), \rho, \epsilon) = 2$  and so the canonization is poor. In the canonization  $c_\infty$  the discontinuities are much more extreme. In this case, we can choose a non-adversarial domain  $K = [-1, 1]$ , and the canonization will be poor for any  $\epsilon > 0$  because the covering number of a set and its closure are the same, and in our case, the closure of  $c_\infty(K)$  will be all of  $K$ .

Figure 1: Visualization of three canonizations for the action of  $\mathbb{G} = \{-1, 1\}$  on  $\mathbb{R}$ . The natural canonization  $c(x) = |x|$ , which is shown to be optimal (Example 3.3), and two discontinuous canonizations, which on an appropriate domain are poor (Example 3.5).



**Example 3.6.** Consider the action of the permutation group  $\mathbb{G} = S_n$  on the space of matrices  $\mathbb{R}^{d \times n}$  by permuting the columns of the matrices. We call such matrices ‘point clouds’. We assume that  $n, d \geq 2$  (the case  $d = 1$  sorting is an isometry by Example 3.3). A natural canonization in this scenario is  $c_{\text{lex}}$ , which permutes the columns of the matrices so that the first row of the matrix is sorted from small to large, and in the event of ties in the first row, sorts according to the second row, and continues in this fashion until a permutation is uniquely defined. The canonization  $c_{\text{lex}}$  is discontinuous. Moreover, the canonization has  $n! = |\mathbb{G}|$  partial limits at any matrix  $M \in \mathbb{R}^{d \times n}$  satisfying that the matrix does not contain two identical columns, but  $M_{1,1} = M_{1,2} = \dots = M_{1,n}$ . Thus, according to Proposition 3.4, for every small enough  $\epsilon > 0$  there exists an adversarial domain for which the canonization is poor.

### Conclusion 2

We show that isometric canonizations are optimal, while discontinuous canonizations can yield poor canonizations. These results give a rigorous justification for the importance of continuous canonizations.

## 4 Case study: Permutation Canonizations

In Example 3.6, we showed that lexicographical sorting is a poor canonization on an adversarial domain. In this section, we analyze the covering numbers of lexicographical sorting when considering

a fixed, ‘natural’ domain of point clouds  $K = [0, 1]^{d \times n}$ . Throughout this section, we will consider the action of the group  $\mathbb{G} = S_n$ , and the distance induced by the element-wise infinity norm  $\rho_\infty(X, Y) = \|X - Y\|_\infty$ . We will show that (for fixed  $\epsilon, d$ ) the covering number of Lexsort grows exponentially in  $n$ , the number of points in the point cloud, while the covering number of the quotient space only grows polynomially in  $n$ . Moreover, we will consider an alternative canonization based on Hilbert curves, and show that its covering numbers also grow only polynomially in  $n$ . The significance of this result is that it gives a theoretical justification for the choice of Point Transformer V3 [30] to use Hilbert canonizations for point cloud serialization.

We begin by proving the exponential growth of Lexsort canonizations:

**Lemma 4.1.** [proof in A.3] *Let  $k, d, n \geq 2$  be natural numbers, and set  $\epsilon = 1/(2k)$ ,  $K = [0, 1]^{d \times n}$  and  $\mathbb{G} = S_n$ . Then the covering number of the lexicographical sorting canonization satisfies*

$$\left(\frac{1}{2\epsilon}\right)^{(d-1) \cdot n + 1} \leq \mathcal{N}(c_{\text{lex}}(K), \rho_\infty, \epsilon). \quad (3)$$

*Proof idea.* The Lexsort canonization is ineffective on the set of its ‘severe discontinuities’- point clouds whose first row is constant. These point clouds form a  $(d - 1) \cdot n + 1$  dimensional hypercube. The covering number of  $c_{\text{lex}}(K)$  is upper bounded by the covering number of this hypercube, which is the left-hand side of (3).  $\square$

Next, we prove that for fixed  $\epsilon, d$ , the quotient space’s covering number grows polynomially in  $n$ :

**Lemma 4.2.** *Let  $n, d$  be natural numbers and  $\epsilon \in (0, 1)$ . Set  $K = [0, 1]^{d \times n}$  and  $\mathbb{G} = S_n$ . Then the covering number of the quotient space satisfies*

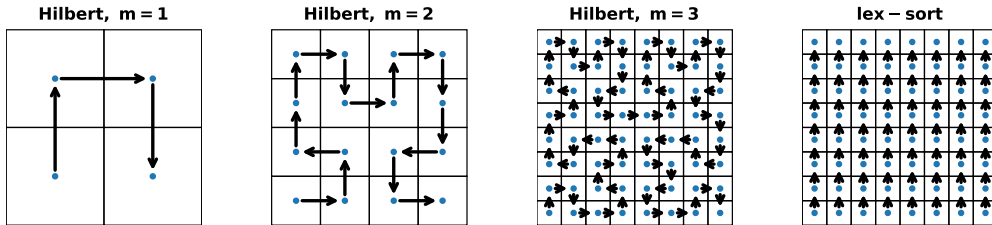
$$\mathcal{N}(K/\mathbb{G}, \rho_{\mathbb{G}}, \epsilon) \leq \binom{n + k^d - 1}{n}, \text{ where } k = \left\lceil \frac{1}{2\epsilon} \right\rceil. \quad (4)$$

*Proof idea.* Set  $k = \lceil 1/(2\epsilon) \rceil$ . The set  $K$  can be covered by  $k^d$  hypercubes of diameter  $k$  and radius  $1/(2k) \leq \epsilon$ . Let  $C$  denote the collection of centers of these hypercubes, and after applying the quotient map  $\pi(c) = [c]$ , we obtain points  $\pi(C)$  in the quotient space which are an  $\epsilon$  cover of  $K/\mathbb{G}$ . Note that points in  $C$  which are permutations of each other are mapped by  $\pi$  to the same orbit. Therefore, the cardinality of the cover  $\pi(C)$  is the number of equivalence classes with respect to the relation on  $C$  defined by the group:  $c_1 \equiv c_2 \iff \exists \pi \in S_n : c_1 = \pi(c_2)$ . As explained in more detail in the proof, the number of equivalence classes is the combinatorial expression in (4).  $\square$

#### 4.1 Hilbert Curve Canonization

Finally, we will provide an intuitive explanation of the Hilbert canonization and formulate the claim that its covering number exhibits only polynomial growth with respect to the point cloud dimensionality. For a full definition of the canonization and proof, see Appendix A.4.

Figure 2: The Hilbert curves  $H_m$  for  $d = 2$  and  $m = 1, 2, 3$  induce an ordering on a grid in  $[0, 1]^d$  with  $2^{2m}$  points. On the right we see the discontinuous Lexsort ordering on the grid.



The Hilbert curve is a space-filling curve, mapping the unit interval  $[0, 1]$  continuously onto a hypercube  $[0, 1]^d$ . It is defined as a limit of curves  $H_m : [0, 1] \rightarrow [0, 1]^d$  which are not onto but

whose image becomes more and more ‘dense’ in  $[0, 1]^d$  as  $m$  grows, as shown in Figure 2 for the case where  $d = 2$ . The curves  $H_m$  can be used to define an order on  $[0, 1]^d$  (at least on points in the image of the curve) and thus induce a canonization. Intuitively, the advantage of this order over the Lexsort ordering is that this ordering is continuous (see Figure 2) again. However, while previous work [30, 6] cited this continuity as justification for Hilbert ordering, a formal justification of why this continuity is important for learning has not yet been provided. We address this caveat by showing the polynomial growth of the covering number of Hilbert canonizations:

**Theorem 4.3.** *Let  $d, n, m \geq 2$  be natural numbers, let  $\epsilon \in (0, 1)$ , and assume that  $\epsilon > 2^{-m-1}$ . Set  $K = [0, 1]^{d \times n}$  and  $\mathbb{G} = S_n$ . Then the covering number of the Hilbert canonization  $c_m$  satisfies*

$$\mathcal{N}(c_m(K), \rho_\infty, \epsilon) \leq \binom{n + \lceil 1/(2\delta) \rceil - 1}{n}, \text{ where } \delta = \frac{(\epsilon - 2^{-m-1})^d}{4}$$

*Proof idea.* When restricting to  $n$ -tuples in  $K$  which are all in the image of  $H_m$ , the Hilbert canonization can be written as  $H_m \circ \text{sort} \circ H_m^{-1}$ . Since  $\text{sort}$  (Proposition 3.3) is an isometry, the image of  $\text{sort} \circ H_m^{-1}$  can be covered efficiently. This cover can then be pushed forward to cover the image of  $H_m \circ \text{sort} \circ H_m^{-1}$ , using the fact that  $H_m$  is Holder continuous.  $\square$

Theorem 4.3 shows that the covering number of the Hilbert canonization grows at worst polynomially in  $n$ , for fixed  $\epsilon > 0$ . This is in contrast with the exponential growth of the sorting canonization, proving a substantial gap between them.

### Conclusion 3

Our analysis proves that the covering number of Hilbert canonizations is far superior to Lexsort canonization, giving a theoretical justification for its superior performance in practice.

To obtain more intuition for the gap between our bounds for the different covering numbers, in Section B.2 in the appendix, we give a table showing these values computed for specific values of  $\epsilon, d, n$ .

## 5 Experiments

We conduct several experiments to verify our theoretical insights and their manifestation in practical learning scenarios. We focus on validating the hierarchy between group averaging, canonization, and non-invariant models (Conclusion 1), and on the hierarchy between Hilbert and Lexsort canonizations (Conclusion 3).

**Coverage on ModelNet** In our first experiment, we considered the ModelNet [31] point cloud classification task. Our first goal was to see whether the covering number hierarchy between the four different methods considered in Table B.2 is preserved when replacing the large domain  $[0, 1]^{3 \times n}$  with the ‘ModelNet point-cloud domain’  $K$ .

As we do not have access to the ‘true point cloud’ domain  $K$ , but only to the train and test sets, we do not compute covering numbers, but a related notion we call the coverage. For given sets  $T$  (representing the test set) and  $R$  (the train set), we define the coverage  $\epsilon(R, T)$  to be the smallest  $\epsilon$  such that  $R$  is an  $\epsilon$  cover of  $T$ . We compute the coverage by choosing, for each test sample  $t \in T$ , the minimum distance from  $t$  to all training samples (for computational efficiency, we consider only samples with the same label as  $t$ ). We call this number  $q_t$ . The coverage is then given by  $\epsilon(R, T) = \max_{t \in T} q_t$ . We call this measure the coverage or *max coverage*. We also consider a more robust measure, the *mean coverage*  $\epsilon_{\text{mean}}(R, T) = \text{mean}\{q_t | t \in \text{Test}\}$ .

We compute the max and mean coverage on ModelNet10 and ModelNet40, using four different distances: (i) the standard Euclidean distance, the Euclidean distance after applying (ii) Lexsort or (iii) Hilbert canonizations to the train and test sets, and (iv) the quotient metric  $d_{\mathbb{G}}$  (in this case, the Wasserstein distance). The results, shown in Table 1, show that the theoretical covering number hierarchy we derived is also preserved when considering coverage of real data: the coverage of  $d_{\mathbb{G}}$  is the lowest, followed by Hilbert, Lexsort, and finally standard Euclidean distance.

Table 1: Estimates of covering number on ModelNet via mean and max coverage, when using Euclidean distances, Lexsort or Hilbert canonizations, and the group distance.

Method	Mean coverage ↓		Max coverage ↓	
	ModelNet10	ModelNet40	ModelNet10	ModelNet40
Euclidean distance	0.4545	0.3821	0.629	0.7304
Lexsort distance	0.3770	0.2988	0.5407	0.5550
Hilbert distance	0.2013	0.1955	0.5283	0.5490
Group distance	<b>0.0917</b>	<b>0.0957</b>	<b>0.2742</b>	<b>0.4880</b>

**Classification on ModelNet** Next, we consider whether the hierarchy in covering numbers between the different methods translates into a corresponding hierarchy in accuracy and generalization error. We choose a simple, purely non-invariant architecture: a Global MLP, and compare the performance of this network (i) without canonization, (ii) with Lexsort canonization, and (iii) with Hilbert canonization (we cannot implement group averaging here since the group is very large). The results, shown in Table 2, reveal that the expected hierarchy is obtained, with Hilbert performing best both on ModelNet40 and ModelNet10, followed by the Lexsort canonization and a plain MLP. The Generalization error column (defined as Test acc.-Train acc.) indicates that this performance gap is due to improved generalization.

Table 2: On the ModelNet classification task, we compare vanilla MLP architectures in three configurations: (a) no canon. (b) Lexsort canon. and (c) Hilbert canon. As predicted by our theory, the Hilbert canon. leads to better generalization, which translates into improved overall accuracy.

Model	ModelNet10		ModelNet40	
	Test Acc ↑	Gen. error ↓	Test Acc ↑	Gen. error ↓
MLP (no canon.)	0.57	0.43	0.442	0.558
MLP (Lexsort)	0.755	0.226	0.693	0.2556
MLP (Hilbert)	<b>0.7815</b>	<b>0.1167</b>	<b>0.74</b>	<b>0.0861</b>

To further verify the generality of our findings, we also trained the three alternatives on smaller samples from the ModelNet40 dataset. We find that the Hilbert > Lexsort > no canon. hierarchy is preserved in all experiments, as shown in Table 9 in the appendix. We note that this experiment is only illustrative; the results attained by simple vanilla MLPs, even with Hilbert canonization, are far from state-of-the-art. In the context of our theory, this can also be explained through the fact that successful models for this task are typically permutation invariant, and hence their generalization is governed by the covering number of the quotient space, which is always better than the covering number of canonizations (Conclusion 1).

We next conduct further experiments to corroborate conclusion 1, which claims that, in terms of generalization, group averaging is preferable to canonizations, which are in turn preferable to ignoring invariance altogether.

**Group averaging on PCA frames** Our first experiment is still with the ModelNet40 classification task, but while the previous experiments investigate canonization w.r.t. permutations, and implicitly relies on the fact that ModelNet models are aligned w.r.t rotations, in this experiment we use the Deepsets [33] model to deal with permutation invariance, and will focus on rotation invariance: we will assume the ModelNet models rotation degree of freedom is initially unknown, and is fixed using the PCA axes as suggested in [23]. Assuming the point cloud singular values are pairwise distinct, this procedure determines the point cloud orientation uniquely up to a  $\{-1, 1\}^3$  symmetry.

We consider four ways to deal with this symmetry: (i) Pure PCA, where the symmetry is ignored (ii) Skewness canonization, where the global sign of the  $x, y$  and  $z$  coordinates is chosen so that their third moment is positive (iii) group averaging and (iv) group augmentation where in each epoch a random group element is applied to the input. This can be seen as an approximation of group averaging. The results of this experiment, detailed in Table 3 demonstrate a clear performance hierarchy. Group averaging achieves the highest overall accuracy, while group augmentation and skewness canonization yield comparable final results, with all three methods significantly outperforming the pure PCA baseline. We note that, as highlighted in Figure 3 in the appendix, the group augmentation approach suffers from a noticeably slower convergence rate compared to the other three methods.

**Group averaging for image classification** Next, we check our approach on image classification. We take the rotated MNIST [15] dataset, and consider the action of the  $p_4$  group, which is the four-element group generated by 90 degree rotations. We consider 4 approaches: simple CNN, the canonization from [14] with random or learned weights (named CN( $p_4$  frozen)-CNN and CN( $p_4$ )-CNN, respectively), and a group average over the 4 elements of the group. As shown in Table 4, the canonizations outperform the simple CNN, but are outperformed by group averaging, as predicted in Conclusion 1. We also see in the table that the accuracy is correlated with the mean coverage of the different methods.

Table 3: *Test accuracy on ModelNet40 with a DeepSets model with orientation determined by PCA, and sign ambiguity handled via averaging, sign augmentation, canonization, or Pure PCA (ignoring the ambiguity).*

Method	Accuracy $\uparrow$
Sign Averaging	<b>0.760</b> $\pm$ 0.0025
Sign Augmentation	0.742 $\pm$ 0.0022
Skewness Canonization	0.742 $\pm$ 0.0050
Pure PCA	0.729 $\pm$ 0.0062

Table 4: *Accuracy and mean coverage on Rotated-MNIST, which is invariant with respect to the group  $p_4$  of 90 rotations. We consider a non-invariant CNN, two canonizations from [14], and group averaging.*

Model	Test Acc. $\uparrow$	Coverage $\downarrow$
CNN	94.8 $\pm$ 0.13	0.185
CN( $p_4$ )-CNN	96.47 $\pm$ 0.24	0.176
CN( $p_4$ frozen)-CNN	95.3 $\pm$ 0.2	0.176
AvgCNN	<b>97.3</b> $\pm$ 0.001	<b>0.167</b>

**Group Averaging for Spectral Embeddings** In the Appendix Section B we present an additional experiment showing the advantage of averaging over previously proposed canonizations, in the context of sign ambiguity present in spectral embeddings for graph learning.

## 6 Conclusion

In this paper, we establish a methodology for comparing different canonizations with group averaging and other invariant models by studying their covering number. We show the covering number of canonizations is at best the covering number of the quotient space (for isometric canonizations), and at worst the covering number of the original domain (for certain discontinuous canonizations). These results suggest that group-averaged models are preferable when computationally feasible. We also show that the covering number of Hilbert canonizations for point clouds is substantially better than that of Lexsort canonizations.

**Limitations and Future Work** A limitation of our analysis is that it relies on upper bounds on the generalization error (Proposition 2.2), which may not be tight. Nonetheless, our experiments indicate that lower covering numbers do correlate with better generalization and learning. Looking towards future developments, a central contribution of this work is the demonstration that a rigorous theoretical comparison between competing canonization methods can be established via their covering numbers. This framework complements the traditional focus on a model’s ability to distinguish between complex symmetric examples, instead highlighting properties that arguably exert a more significant influence on the ultimate success of the learning process. In future work, we intend to apply our framework to other canonizations and extend it to enable a rigorous treatment of the generalization of frame averaging.

## 7 Acknowledgments

All authors are funded by Israeli Science Foundation grant no.272/23. N.D. and S.H. wish to thank Jonathan W Siegel and Hannah Lawrence for many interesting discussions related to the topics presented in the paper.

## References

- [1] Josep Arús-Pous, Simon V. Johansson, Oleksii Prykhodko, Esben J. Bjerrum, Christian Tyrchan, Jean-Louis Reymond, Hongming Chen, and Ola Engkvist. Randomized SMILES strings improve the quality of molecular generative models. *Journal of Cheminformatics*, 11(1):71, 2019.
- [2] Justin Baker, Shih-Hsin Wang, Tommaso De Fernex, and Bao Wang. An explicit frame construction for normalizing 3D point clouds. In Ruslan Salakhutdinov, Zico Kolter, Katherine Heller, Adrian Weller, Nuria Oliver, Jonathan Scarlett, and Felix Berkenkamp, editors, *Proceedings of the 41st International Conference on Machine Learning*, volume 235 of *Proceedings of Machine Learning Research*, pages 2456–2473. PMLR, 21–27 Jul 2024.
- [3] Esben Jannik Bjerrum. Smiles enumeration as data augmentation for neural network modeling of molecules. *ArXiv*, abs/1703.07076, 2017.
- [4] Sergey Bobkov and Michel Ledoux. *One-dimensional empirical measures, order statistics, and Kantorovich transport distances*, volume 261. American Mathematical Society, 2019.
- [5] Johann Brehmer, Sönke Behrends, Pim de Haan, and Taco Cohen. Does equivariance matter at scale?, 2025.
- [6] Wanli Chen, Xinge Zhu, Guojin Chen, and Bei Yu. Efficient point cloud analysis using hilbert curve. In Shai Avidan, Gabriel Brostow, Moustapha Cissé, Giovanni Maria Farinella, and Tal Hassner, editors, *Computer Vision – ECCV 2022*, pages 730–747, Cham, 2022. Springer Nature Switzerland.
- [7] Nadav Dym, Hannah Lawrence, and Jonathan W Siegel. Equivariant frames and the impossibility of continuous canonicalization. In *International Conference on Machine Learning*, pages 12228–12267. PMLR, 2024.
- [8] Bryn Elesedy. Provably strict generalisation benefit for invariance in kernel methods. In A. Beygelzimer, Y. Dauphin, P. Liang, and J. Wortman Vaughan, editors, *Advances in Neural Information Processing Systems*, 2021.
- [9] Billy J Franks, Christopher Morris, Ameya Velinger, and Floris Geerts. Weisfeiler-leman at the margin: when more expressivity matters. In *Proceedings of the 41st International Conference on Machine Learning*, pages 13885–13926, 2024.
- [10] Benjy Friedmann and Michael Werman. Canonnet: Canonical ordering and curvature learning for point cloud analysis, 2025.
- [11] Zhijian He and Art B Owen. Extensible grids: uniform sampling on a space filling curve. *Journal of the Royal Statistical Society: Series B (Statistical Methodology)*, 78(4):917–931, 2016.
- [12] Snir Hordan, Maya Bechler-Speicher, Gur Lifshitz, and Nadav Dym. Spectral graph neural networks are incomplete on graphs with a simple spectrum. *arXiv preprint arXiv:2506.05530*, 2025.
- [13] Michael Ito, Danai Koutra, and Jenna Wiens. Random search neural networks for efficient and expressive graph learning. In *The Thirty-ninth Annual Conference on Neural Information Processing Systems*, 2026.
- [14] Sékou-Oumar Kaba, Arnab Kumar Mondal, Yan Zhang, Yoshua Bengio, and Siamak Ravanbakhsh. Equivariance with learned canonicalization functions. In *International Conference on Machine Learning*, pages 15546–15566. PMLR, 2023.
- [15] Hugo Larochelle, Dumitru Erhan, Aaron Courville, James Bergstra, and Yoshua Bengio. An empirical evaluation of deep architectures on problems with many factors of variation. In *Proceedings of the 24th international conference on Machine learning*, pages 473–480, 2007.
- [16] Ya-Wei Eileen Lin and Ron Levie. Adaptive canonicalization with application to invariant anisotropic geometric networks. In *The Fourteenth International Conference on Learning Representations*, 2026.

- [17] Yuchao Lin, Jacob Helwig, Shurui Gui, and Shuiwang Ji. Equivariance via minimal frame averaging for more symmetries and efficiency. In *Forty-first International Conference on Machine Learning*, 2024.
- [18] George Ma, Yifei Wang, Derek Lim, Stefanie Jegelka, and Yisen Wang. A canonicalization perspective on invariant and equivariant learning. In *The Thirty-eighth Annual Conference on Neural Information Processing Systems*, 2024.
- [19] George Ma, Yifei Wang, Derek Lim, Stefanie Jegelka, and Yisen Wang. A canonicalization perspective on invariant and equivariant learning. *Advances in Neural Information Processing Systems*, 37:60936–60979, 2024.
- [20] George Ma, Yifei Wang, and Yisen Wang. Laplacian canonization: A minimalist approach to sign and basis invariant spectral embedding. In *Thirty-seventh Conference on Neural Information Processing Systems*, 2023.
- [21] Sohir Maskey, Gitta Kutyniok, and Ron Levie. Generalization bounds for message passing networks on mixture of graphons. *SIAM Journal on Mathematics of Data Science*, 7(2):802–825, 2025.
- [22] Mircea Petrache and Shubhendu Trivedi. Approximation-generalization trade-offs under (approximate) group equivariance. In *Thirty-seventh Conference on Neural Information Processing Systems*, 2023.
- [23] Omri Puny, Matan Atzmon, Heli Ben-Hamu, Ishan Misra, Aditya Grover, Edward J Smith, and Yaron Lipman. Frame averaging for invariant and equivariant network design. *arXiv preprint arXiv:2110.03336*, 2021.
- [24] Jonathan W. Siegel, Snir Hordan, Hannah Lawrence, Ali Syed, and Nadav Dym. Quantitative approximation rates for group equivariant learning, 2026.
- [25] Richard P Stanley. Enumerative combinatorics volume 1 second edition. *Cambridge studies in advanced mathematics*, 2011.
- [26] Behrooz Tahmasebi and Stefanie Jegelka. Generalization bounds for canonicalization: A comparative study with group averaging. In *The Thirteenth International Conference on Learning Representations*, 2025.
- [27] Behrooz Tahmasebi and Stefanie Jegelka. Regularity in canonicalized models: A theoretical perspective. In *International Conference on Artificial Intelligence and Statistics*, pages 4789–4797. PMLR, 2025.
- [28] Antonis Vasileiou, Stefanie Jegelka, Ron Levie, and Christopher Morris. Survey on generalization theory for graph neural networks. *arXiv preprint arXiv:2503.15650*, 2025.
- [29] David Weininger, Arthur Weininger, and Joseph L. Weininger. Smiles. 2. algorithm for generation of unique smiles notation. *J. Chem. Inf. Comput. Sci.*, 29:97–101, 1989.
- [30] Xiaoyang Wu, Li Jiang, Peng-Shuai Wang, Zhijian Liu, Xihui Liu, Yu Qiao, Wanli Ouyang, Tong He, and Hengshuang Zhao. Point transformer v3: Simpler, faster, stronger. In *CVPR*, 2024.
- [31] Zhirong Wu, Shuran Song, Aditya Khosla, Fisher Yu, Linguang Zhang, Xiaoou Tang, and Jianxiong Xiao. 3d shapenets: A deep representation for volumetric shapes. In *Proceedings of the IEEE conference on computer vision and pattern recognition*, pages 1912–1920, 2015.
- [32] Huan Xu and Shie Mannor. Robustness and generalization. *Machine learning*, 86(3):391–423, 2012.
- [33] Manzil Zaheer, Satwik Kottur, Siamak Ravanbakhsh, Barnabas Poczos, Russ R Salakhutdinov, and Alexander J Smola. Deep sets. *Advances in neural information processing systems*, 30, 2017.
- [34] Cai Zhou, Zijie Chen, Zian Li, Jike Wang, Kaiyi Jiang, Pan Li, Rose Yu, Muhan Zhang, Stephen Bates, and Tommi Jaakkola. Rethinking diffusion models with symmetries through canonicalization with applications to molecular graph generation, 2026.

## A Proofs

In this section, we provide the proofs that are missing in the main text.

### A.1 Generalization and Covering Numbers

Our generalization results are based on the results of [32]: a combination of Theorem 1 and Example 4 from [32] yields the following theorem:

**Theorem A.1** ([32]). *If  $X$  is compact w.r.t. metric  $\rho$ , and  $l(h_S, \cdot)$  is Lipschitz continuous with Lipschitz constant  $c(s)$ , i.e.,*

$$|l(h_S, x_1) - l(h_S, x_2)| \leq c(S)\rho(x_1, x_2), \quad \forall x_1, x_2 \in X,$$

*and the training sample set  $S$  is generated by  $n$  IID draws from  $\mu$ , then for any  $\delta, \epsilon > 0$ , with probability at least  $1 - \delta$  we have*

$$|\mathcal{L}_{\text{exp}}(h_S) - \mathcal{L}_{\text{emp}}(h_S)| \leq 2c(S)\epsilon + M\sqrt{\frac{2\mathcal{N}(X, \rho, \epsilon) \ln 2 + 2 \ln(1/\delta)}{n}}. \quad (5)$$

We now explain how Theorem 2.1 from the main text follows from Theorem A.1. We recall Theorem 2.1:

**Theorem 2.1.** *[Proof in Appendix A.1, based on [32]] Let  $(X, \rho)$  and  $(Y, \rho_Y)$  be metric spaces and assume  $X$  is compact. Let  $f : X \rightarrow Y$  be a  $c_f$  Lipschitz function, and let  $\ell : Y \times Y \rightarrow [0, M]$  be a  $c_\ell$  Lipschitz function. Then for any  $\epsilon, \delta > 0$  and natural  $n$ , for a training sample set  $S$  generated by  $n$  IID draws from a distribution  $\mu$ , with probability of at least  $1 - \delta$ , we have*

$$|\mathcal{L}_{\text{exp}}(h_S) - \mathcal{L}_{\text{emp}}(h_S)| \leq 2c_\ell(c_{h_S} + c_f)\epsilon + M\sqrt{\frac{2\mathcal{N}(X, \rho, \epsilon) \ln 2 + 2 \ln(1/\delta)}{n}}$$

where  $c_{h_S}$  denotes the Lipschitz constant of  $h_S$ .

*Proof.* We will apply Theorem A.1, where to apply it to the setting discussed in Theorem 2.1, we set

$$l(h_S, x) = \ell(h_S(x), f(x)).$$

We note that  $l$  is Lipschitz with a Lipschitz constant of  $c_\ell(c_{h_S} + c_f)$  as the following shows:

$$\begin{aligned} |l(h_S, x) - l(h_S, x')| &= |\ell(h_S(x), f(x)) - \ell(h_S(x'), f(x'))| \\ &\leq c_\ell(\rho_Y(h_S(x), h_S(x')) + \rho_Y(f(x), f(x'))) \\ &\leq c_\ell(c_{h_S}\rho(x, x') + c_f \cdot \rho(x, x')) \\ &= c_\ell(c_{h_S} + c_f)(\rho(x, x')) \end{aligned}$$

Now, to conclude the proof, choose any  $\epsilon, \delta > 0$ . Since  $l$  is  $c_\ell(c_{h_S} + c_f)$  Lipschitz, we have

$$|\mathcal{L}_{\text{exp}}(h_S) - \mathcal{L}_{\text{emp}}(h_S)| \stackrel{(5)}{\leq} 2c_\ell(c_{h_S} + c_f)\epsilon + M\sqrt{\frac{2\mathcal{N}(X, \rho, \epsilon) \ln 2 + 2 \ln(1/\delta)}{n}}$$

which proves Theorem 2.1. □

Next, we prove Proposition 2.2.

**Proposition 2.2.** *[Proof in Appendix A.1] Let  $(K, \rho, \mathbb{G})$  be a module. Let  $(Y, \rho_Y)$  be a metric space, and assume  $K$  is compact. Let  $f : K \rightarrow Y$  be a  $c_f$  Lipschitz function **which is  $\mathbb{G}$  invariant**, and let  $\ell : Y \times Y \rightarrow [0, M]$  be a  $c_\ell$  Lipschitz function, then for any  $\epsilon, \delta > 0$  and natural  $n$ , for a training sample set  $S$  generated by  $n$  IID draws from the distribution  $\mu$ , with probability of at least  $1 - \delta$ , we have*

$$|\mathcal{L}_{\text{exp}}(h_S) - \mathcal{L}_{\text{emp}}(h_S)| \leq 2c_\ell(c_{h_S} + c_f)\epsilon + M\sqrt{\frac{2\mathcal{N}(h_S) \ln 2 + 2 \ln(1/\delta)}{n}}$$

where

$$\mathcal{N}(h_S) = \begin{cases} \mathcal{N}(K, \rho, \epsilon) & \text{if } h_S \text{ is } c_{h_S} \text{ Lipschitz} \\ \mathcal{N}(c(K), \rho, \epsilon) & \text{if } h_S = \tilde{h}_S \circ c, \tilde{h}_S \text{ is } c_{h_S} \text{ Lipschitz, and } c \text{ is a canon.} \\ \mathcal{N}(K/\mathbb{G}, \rho_{\mathbb{G}}, \epsilon) & \text{if } h_S \text{ is } c_{h_S} \text{ Lipschitz and } \mathbb{G} \text{ invariant} \end{cases} \quad (1)$$

*Proof.* The first case where  $h_S$  is Lipschitz (but not invariant) follows directly from Theorem 2.1.

Next, we consider the second case  $h_S = \tilde{h}_S \circ c$ , where  $\tilde{h}_S$  is  $c_{h_S}$  Lipschitz. We note that since  $\tilde{h}_S$  operates on  $c(S)$ , we can think of it as defined by the set  $\tilde{S} = c(S)$ , and so we can write  $\tilde{h}_S := \tilde{h}_{\tilde{S}}$ . This notation is more convenient for the proof.

We want to consider the domain to be  $c(K)$ , so consider the following distribution measure on  $c(K)$ :

$$\tilde{\mu}(A) = \mu(c^{-1}(A))$$

Note that

$$\forall x \in c(K), h_S(x) = \tilde{h}_{\tilde{S}}(x)$$

Next, for any fixed  $n$  samples from  $K$ , which we denote by  $S = \{x_1, x_2, \dots, x_n\}$ , denote its image by  $\tilde{S} = \{c(x_1), \dots, c(x_n)\}$ . Then

$$\mathcal{L}_{\text{emp}}(h_S) = \frac{1}{n} \sum_{i=1}^n \ell(\tilde{h}_{\tilde{S}}(c(x_i)), f(x_i)) = \frac{1}{n} \sum_{i=1}^n \ell(\tilde{h}_{\tilde{S}}(c(x_i)), f(c(x_i))) = \mathcal{L}_{\text{emp}}(\tilde{h}_{\tilde{S}})$$

So, the empirical losses are the same, and next we show the expected losses are the same:

$$\begin{aligned} \mathcal{L}_{\text{exp}}(\tilde{h}_{\tilde{S}}) &= \mathbb{E}_{x \sim \tilde{\mu}} \ell(\tilde{h}_{\tilde{S}}(x), f(x)) = \int_{c(K)} \ell(\tilde{h}_{\tilde{S}}(x), f(x)) d\tilde{\mu} = \int_K \ell(\tilde{h}_{\tilde{S}}(c(x)), f(c(x))) d\mu \\ &= \int_K \ell(h_S(x), f(x)) d\mu = \mathcal{L}_{\text{exp}}(h_S) \end{aligned}$$

Finally, we apply Theorem 2.1 on  $\tilde{h}_{\tilde{S}}$  and as it's  $c_{h_S}$  lipschiz we obtain that with probability at least  $1 - \delta$ , according to  $\tilde{\mu}$ , it holds that:

$$|\mathcal{L}_{\text{exp}}(\tilde{h}_{\tilde{S}}) - \mathcal{L}_{\text{emp}}(\tilde{h}_{\tilde{S}})| \leq 2c_{\ell}(c_{h_S} + c_f)\epsilon + M \sqrt{\frac{2\mathcal{N}(c(K), \rho_X, \epsilon) \ln 2 + 2 \ln(1/\delta)}{n}}$$

Let us abbreviate the right hand side of the equation above by  $\eta = 2c_{\ell}(c_{h_S} + c_f)\epsilon + M \sqrt{\frac{2\mathcal{N}(c(K), \rho_X, \epsilon) \ln 2 + 2 \ln(1/\delta)}{n}}$ . We then have

$$\begin{aligned} 1 - \delta &\leq \mathbb{P}_{\tilde{\mu}}\{\tilde{S} \subseteq c(K) \mid |\mathcal{L}_{\text{exp}}(\tilde{h}_{\tilde{S}}) - \mathcal{L}_{\text{emp}}(\tilde{h}_{\tilde{S}})| \leq \eta\} \\ &= \mathbb{P}_{\mu}\{S = (x_1, \dots, x_n) \mid |\mathcal{L}_{\text{exp}}(\tilde{h}_{\tilde{S}} \circ c) - \mathcal{L}_{\text{emp}}(\tilde{h}_{\tilde{S}} \circ c)| \leq \eta\} \\ &= \mathbb{P}_{\mu}\{S = (x_1, \dots, x_n) \mid |\mathcal{L}_{\text{exp}}(h_S) - \mathcal{L}_{\text{emp}}(h_S)| \leq \eta\} \end{aligned}$$

which concludes the proof of the second case.

In the third case, where  $h_S$  is  $c_{h_S}$  lipshiz and invariant, we want to consider the domain  $K/\mathbb{G}$  and define  $\pi : K \rightarrow K/\mathbb{G}$  by  $\pi(k) = [k]$ . Define the following distribution on  $K/\mathbb{G}$  by:

$$\tilde{\mu}(A) = \mu(\pi^{-1}(A))$$

Define  $\tilde{S} = \pi(S)$  and

$$\tilde{h}_{\tilde{S}}, \tilde{f} : k/\mathbb{G} \rightarrow \mathbb{R}$$

by

$$\tilde{h}_{\tilde{S}}([x]) = h_S(x), \tilde{f}([x]) = f(x)$$

Note that by invariance, these functions are well defined. Next, for any set  $S$  of  $n$  samples  $x_1, x_2, \dots, x_n$  from  $K$ , denote  $\tilde{S} = \{\pi(x_1), \dots, \pi(x_n)\}$ , then

$$\mathcal{L}_{\text{emp}}(h_S) = \frac{1}{n} \sum_{i=1}^n \ell(h_S(x_i), f(x_i)) = \frac{1}{n} \sum_{i=1}^n \ell(\tilde{h}_{\tilde{S}}(\pi(x_i)), \tilde{f}(\pi(x_i))) = \mathcal{L}_{\text{emp}}(\tilde{h}_{\tilde{S}})$$

So, the empirical losses are the same, and next we show the expected losses:

$$\begin{aligned}\mathcal{L}_{\text{exp}}(\tilde{h}_{\tilde{S}}) &= \mathbb{E}_{x \sim \tilde{\mu}} \ell(\tilde{h}_{\tilde{S}}(x), \tilde{f}(x)) = \int_{K/\mathbb{G}} \ell(\tilde{h}_{\tilde{S}}(x), \tilde{f}(x)) d\tilde{\mu}(x) = \int_K \ell(\tilde{h}_S(\pi(x)), \tilde{f}(\pi(x))) d\mu \\ &= \int_K \ell(h_S(x), f(x)) d\mu = \mathcal{L}_{\text{exp}}(h_S)\end{aligned}$$

Note that  $\tilde{f}$  is  $c_f$  Lipschitz function and  $\tilde{h}_S$  is  $c_{h_S}$  Lipschitz function (see Lemma 20 in [24]). Therefore, we can apply Theorem 2.1 on  $\tilde{h}_S$  and  $\tilde{f}$  and we obtain that with probability at least  $1 - \delta$  it holds that:

$$|\mathcal{L}_{\text{exp}}(\tilde{h}_S) - \mathcal{L}_{\text{emp}}(\tilde{h}_S)| \leq 2c_\ell(c_{h_S} + c_f)\epsilon + M\sqrt{\frac{2\mathcal{N}(K/\mathbb{G}, \rho_{\mathbb{G}}, \epsilon) \ln 2 + 2 \ln(1/\delta)}{n}}$$

And as  $|\mathcal{L}_{\text{exp}}(\tilde{h}_{\tilde{S}}) - \mathcal{L}_{\text{emp}}(\tilde{h}_{\tilde{S}})| = |\mathcal{L}_{\text{exp}}(h_S) - \mathcal{L}_{\text{emp}}(h_S)|$  (see the more formal argument used for bounding the generalization of  $h_S \circ c$ ) we obtain that with probability of at least  $1 - \delta$ ,

$$|\mathcal{L}_{\text{exp}}(h_S) - \mathcal{L}_{\text{emp}}(h_S)| \leq 2c_\ell(c_{h_S} + c_f)\epsilon + M\sqrt{\frac{2\mathcal{N}(k/\mathbb{G}, \rho_{\mathbb{G}}, \epsilon) \ln 2 + 2 \ln(1/\delta)}{n}}$$

□

We next state and prove a result mentioned in the main text: that the Lipschitz constant of a backbone model is preserved under averaging

**Proposition A.2.** *Let  $(X, \rho, \mathbb{G})$  be a module, and assume that  $\mathbb{G}$  is a compact group with a Haar probability measure  $\mu$ . Let  $Y$  be a normed space and assume that  $h : X \rightarrow Y$  is  $c_h$  Lipschitz. Then the averaged function*

$$q(x) = \int_{\mathbb{G}} h(gx) d\mu(g)$$

is  $c_h$  Lipschitz as well.

*Proof.* For every  $x_1, x_2 \in X$

$$\begin{aligned}\|q(x_1) - q(x_2)\| &= \left\| \int_{\mathbb{G}} h(gx_1) d\mu(g) - \int_{\mathbb{G}} h(gx_2) d\mu(g) \right\| \\ &\stackrel{\text{Jensen}}{\leq} \int_{\mathbb{G}} \|h(gx_1) - h(gx_2)\| d\mu(g) \\ &\leq \int_{\mathbb{G}} c_h \rho(gx_1, gx_2) d\mu(g) \\ &= \int_{\mathbb{G}} c_h \rho(x_1, x_2) d\mu(g) \\ &= c_h \rho(x_1, x_2)\end{aligned}$$

□

## A.2 Proofs for Section 3

We restate and prove Proposition 2.4.

**Proposition 2.4.** *[See proof in A.2] Let  $(K, \rho, \mathbb{G})$  be a module, and assume  $\mathbb{G}$  is finite. Then*

$$\mathcal{N}(K, \rho, \epsilon) \leq |\mathbb{G}| \cdot \mathcal{N}(K/\mathbb{G}, \rho_{\mathbb{G}}, \epsilon).$$

*Proof.* Let  $C$  be an  $\epsilon$ -cover of  $K/\mathbb{G}$  under  $\rho_{\mathbb{G}}$ , and define

$$\hat{C} := \{g \cdot y \mid y \in C, g \in \mathbb{G}\}.$$

Then of course  $|\hat{C}| \leq |\mathbb{G}| \cdot |C|$ .

We claim that  $\widehat{C}$  is an  $\epsilon$ -cover of  $K$  under  $d$ . Let  $x \in K$ . Since  $C$  covers  $K/\mathbb{G}$ , there exists  $y \in C$  such that

$$\rho_{\mathbb{G}}([x], [y]) \leq \epsilon.$$

Because  $\mathbb{G}$  is finite, the minimum in the definition of  $\rho_{\mathbb{G}}$  is attained, so there exists  $g \in \mathbb{G}$  such that

$$\rho(x, g \cdot y) \leq \epsilon.$$

By construction,  $g \cdot y \in \widehat{C}$ , hence  $\widehat{C}$  covers  $K$ . Therefore  $\mathcal{N}(K, \rho, \epsilon) \leq |\widehat{C}| \leq |\mathbb{G}| \cdot |C| = |\mathbb{G}| \cdot \mathcal{N}(K/\mathbb{G}, \rho_{\mathbb{G}}, \epsilon)$ .  $\square$

We next prove Proposition 3.2.

**Proposition 3.2.** *[proof in A.2] Any isometric canonization  $c : K \rightarrow K$  is  $(K, \epsilon)$  optimal for all  $\epsilon > 0$ .*

*Proof.* As it always holds that

$$\mathcal{N}(K/\mathbb{G}, \rho_{\mathbb{G}}, \epsilon) \leq \mathcal{N}(c(K), \rho, \epsilon)$$

we just need to prove the opposite direction.

Let  $C$  be a cover of  $K/\mathbb{G}$  with  $\mathcal{N}(K/\mathbb{G}, \rho, \epsilon)$  elements. Consider

$$\widehat{C} := \{c(x) | x \in C\}$$

and we will prove that  $\widehat{C}$  is an  $\epsilon$  cover of  $c(K)$ .

Let  $y \in c(K)$ , then by definition  $\exists x \in K : y = c(x)$ . By the definition of cover  $\exists z \in C$  such that  $\rho([x], [z]) \leq \epsilon$ . But as  $\rho_{\mathbb{G}}([x], [z]) = \rho(c(x), c(z))$  we obtain that  $\rho(y, c(z)) \leq \epsilon$ . So  $\widehat{C}$  is an  $\epsilon$  cover of  $c(K)$  as desired.  $\square$

**Example 3.3.** The following canonizations are isometries (see proof in A.2)

1. The canon.  $c(x) = |x|$  with respect to the action of  $\{-1, 1\}$  on  $\mathbb{R}$  and the standard metric.
2. The canon.  $\text{sort} : \mathbb{R}^n \rightarrow \mathbb{R}^n$  with respect to the action of permutations and a metric  $\rho$  induced by a  $p$  norm.
3. The centralization canon. defined for point clouds in  $\mathbb{R}^{d \times n}$  with respect to the action of translation by vectors in  $\mathbb{R}^d$ , with the metric  $\rho$  induced by the Frobenius norm.

*Proof.* The canonization  $c(x) = |x|$  is an isometry as

$$\forall x, y \in K, \rho_{\mathbb{G}}([x], [y]) = \min\{|x - y|, |x + y|\} = ||x| - |y|| = |c(x) - c(y)|$$

The fact that sorting is an isometry with respect to the metric  $\rho_{\mathbb{G}}$  induced from a  $p$  norm (which is the  $p$ -Wasserstein metric) is shown in Lemma 4.2 in [4].

consider the action of  $\mathbb{R}^d$  on  $\mathbb{R}^{d \times n}$  by translating all columns of a matrix in  $\mathbb{R}^{d \times n}$  by a vector in  $\mathbb{R}^d$ . Let  $\rho$  be the metric induced from the Frobenius norm  $\rho(X, Y) = \|X - Y\|_F$ , and let  $c$  be the centralization mapping  $c(X) = X - \frac{1}{n}X1_{n \times n}$ . This mapping is a canonization and an isometry. To see it is an isometry, note that we have for any canonization  $\rho(c(X), c(Y)) \leq \rho_{\mathbb{G}}([X], [Y])$ , and we get the converse inequality by noting that  $c$  is the orthogonal projection from the inner product space  $\mathbb{R}^{d \times n}$  onto the subspace  $\{X \in \mathbb{R}^{d \times n} \mid X1_{n \times n} = 0\}$ . Thus, let  $g \in \mathbb{G}$  be a translation vector such that  $\rho_{\mathbb{G}}([X], [Y]) = \rho(X, gY)$ . Then

$$\rho_{\mathbb{G}}([X], [Y]) = \rho(X, gY) = \|X - gY\|_F \leq \|c(X) - c(gY)\|_F = \|c(X) - c(Y)\|_F = \rho(c(X), c(Y))$$

$\square$

We next formulate and prove a result mentioned in the main text

**Proposition A.3.** *Let  $(K, \rho, \mathbb{G})$  be a module, and  $c : K \rightarrow K$  a canonization. Then  $c$  is an isometric canonization if and only if  $c$  is 1-Lipschitz.*

*Proof.* Assume  $c$  is an isometric canonization. Recall that this means that  $\rho(c(x), c(y)) = \rho_{\mathbb{G}}([x], [y])$ . This implies that  $c$  is Lipschitz because

$$\rho(c(x), c(y)) = \rho_{\mathbb{G}}([x], [y]) \leq \rho(x, y), \quad \forall x, y \in K$$

In the other direction, assume that  $c$  is 1-Lipschitz. This implies that for all  $g \in \mathbb{G}$

$$\rho(c(x), c(y)) = \rho(c(gx), c(y)) \leq \rho(gx, y).$$

Since this is true for all  $g \in G$ , we can minimize over  $g$  and obtain the inequality  $\rho(c(x), c(y)) \leq \rho_{\mathbb{G}}([x], [y])$ . The converse of this inequality is always true for any canonization, namely

$$\rho(c(x), c(y)) \geq \rho_{\mathbb{G}}([x], [y])$$

and so we obtain that  $c$  is an isometric canonization.  $\square$

We restate and prove 3.4.

**Proposition 3.4.** *[proof in A.2] Let  $(V, \rho, \mathbb{G})$  be a module, where  $\mathbb{G}$  is a finite group. Let  $c$  be a canonization that has  $|\mathbb{G}|$  partial limits at a point  $x \in V$ . Then for any small enough  $\epsilon > 0$  there exists a  $\mathbb{G}$  invariant set  $K \subseteq V$  such that  $\mathcal{N}(c(K), \rho, \epsilon) = \mathcal{N}(K, \rho, \epsilon) = |\mathbb{G}| \cdot \mathcal{N}(K/\mathbb{G}, \rho, \epsilon)$ .*

*Proof.*  $L$  is a partial limit of  $c$  if there is a sequence  $x_n \rightarrow x$  such that  $c(x_n) \rightarrow L$ . We claim that  $L$  must be in the orbit of  $x$ . Indeed,  $c(x_n) = g_n x_n$  for appropriate  $g_n \in G$ . Since  $\mathbb{G}$  is finite, by passing to a subsequence, we can assume that  $g_n = g \in G$  does not depend on  $n$ . Since  $x \mapsto gx$  is an isometry, we know that  $g x_n \rightarrow gx = L$ . In particular,  $gx \neq x$  for every  $g \neq e$ . Choose some  $\epsilon < \min_{g \neq e} |x - g \cdot x|$ , and define the  $G$  invariant set  $K = K(\epsilon)$  by  $K := \cup_{g \in G} B(g \cdot x, \epsilon)$ . Note that  $c(K)$  contains all partial limits of  $c$  at  $x$ , and therefore  $gx \in c(K)$  for all  $g \in G$ . Since the distance between any two elements in the orbit of  $x$  is larger than  $\epsilon$ , an  $\epsilon$  cover of  $c(K)$  must contain at least  $|\mathbb{G}|$  elements. On the other hand,  $K$  itself is a union of  $|\mathbb{G}|$  balls of radius  $\epsilon$ , and therefore

$$\mathcal{N}(c(K), \rho, \epsilon) \leq \mathcal{N}(K, \rho, \epsilon) \leq |\mathbb{G}| \leq \mathcal{N}(c(K), \rho, \epsilon),$$

and therefore all these inequalities are equalities and the covering number is exactly  $|\mathbb{G}|$ .

Finally, note that  $\rho(K/G, \rho_G, \epsilon) = 1$  as one ball of radius  $\epsilon$  is enough for covering the quotient space, as all  $|\mathbb{G}|$  balls are the same up to group action.  $\square$

### A.3 Proofs for Section 4

For proving Lemma 4.2, we need the following lemma:

**Lemma A.4.** *Let  $S := [m]^n$  all vectors with  $n$  elements, each between 1 and  $m$ . Define two vectors  $v \equiv u \iff \exists \pi \in S_n : u = \pi \cdot v$ . Then the number of equivalent classes is exactly  $\binom{n+m-1}{n}$ .*

*Proof.* Define  $\forall i \in [m], c_i^u$  to be the number of times  $i$  appears in  $u$ .

Note that  $u \equiv v \iff \forall i \in [m] : c_i^u = c_i^v$ . So we want to ask how many solutions there are to the following system:

$$\begin{aligned} \sum_{i=1}^m c_i &= n \\ \forall i, c_i &\geq 0 \end{aligned}$$

By [25] we know the number of solutions to the equation is  $\binom{n+m-1}{n}$ .  $\square$

We now restate and prove 4.2.

**Lemma 4.2.** *Let  $n, d$  be natural numbers and  $\epsilon \in (0, 1)$ . Set  $K = [0, 1]^{d \times n}$  and  $\mathbb{G} = S_n$ . Then the covering number of the quotient space satisfies*

$$\mathcal{N}(K/\mathbb{G}, \rho_{\mathbb{G}}, \epsilon) \leq \binom{n + k^d - 1}{n}, \quad \text{where } k = \left\lceil \frac{1}{2\epsilon} \right\rceil. \quad (4)$$

*Proof.* Set  $k = \lceil 1/(2\epsilon) \rceil$ . The set  $K$  can be covered by  $k^d$  hypercubes of diameter  $k$  and radius  $1/(2k) \leq \epsilon$ . Let  $C$  denote the collection of centers of these hypercubes, namely

$$C = \left\{ \left[ \frac{2i_1 + 1}{2k}, \frac{2i_2 + 1}{2k}, \dots, \frac{2i_n + 1}{2k} \right] \mid i_j \in \{0, 1, \dots, k-1\}, 1 \leq j \leq n \right\}.$$

Applying the quotient map  $\pi(c) = [c]$  we obtain points  $\pi(C)$  in the quotient space which are an  $\epsilon$  cover of  $K/\mathbb{G}$ . Note that points in  $C$  which are permutations of each other are mapped by  $\pi$  to the same orbit. Therefore, the cardinality of the cover  $\pi(C)$  is the number of equivalence classes with respect to the relation on  $C$  defined by the group:  $c_1 \equiv c_2 \iff \exists \pi \in S_n : c_1 = \pi(c_2)$ . Using Lemma A.4, we know that the number of equivalence classes is

$$|\pi(C)| = \binom{n + k^d - 1}{n}$$

□

We now restate and prove 4.1.

**Lemma 4.1.** [proof in A.3] *Let  $k, d, n \geq 2$  be natural numbers, and set  $\epsilon = 1/(2k)$ ,  $K = [0, 1]^{d \times n}$  and  $\mathbb{G} = S_n$ . Then the covering number of the lexicographical sorting canonization satisfies*

$$\left( \frac{1}{2\epsilon} \right)^{(d-1) \cdot n + 1} \leq \mathcal{N}(c_{\text{lex}}(K), \rho_\infty, \epsilon). \quad (3)$$

*Proof.* We consider the set  $U \subset [0, 1]^{d \times n}$  defined by

$$U = \{X \in [0, 1]^{d \times n} \mid X_{11} = X_{12} = \dots = X_{1n}\}$$

The set  $U$  is not a subset of  $c_{\text{lex}}(K)$ , but it is a subset of its closure  $\overline{c_{\text{lex}}(K)}$ . This is because for every  $X \in U$  we can apply an arbitrarily small perturbation of the first row of  $X$  so that it is ordered from small to large, and the  $X$  will be unaffected by the canonization. We then obtain

$$\mathcal{N}(c_{\text{lex}}(K), \rho, \epsilon) = \mathcal{N}(\overline{c_{\text{lex}}(K)}, \rho, \epsilon) \geq \mathcal{N}(U, \rho, \epsilon) \stackrel{(*)}{=} \left( \frac{1}{2\epsilon} \right)^{(d-1) \cdot n + 1},$$

where  $(*)$  follows from the fact that the hypercube  $[0, 1]^{(d-1) \cdot n + 1}$  can be mapped isometrically (in the  $\infty$  norm) to  $U$  via  $f : [0, 1]^{(d-1) \cdot n + 1} \rightarrow U$  by repeating the first entry  $n - 1$  times, obtaining an  $n \cdot d$  vector, and then transposing to be of shape  $n \times d$ , and from the fact that the covering number of the hypercube is  $\left( \frac{1}{2\epsilon} \right)^{(d-1) \cdot n + 1}$ . □

#### A.4 Hilbert Canonization

In this appendix, we give a formal definition of Hilbert curves and a full proof of Theorem 4.3.

The Hilbert curve  $H(x)$  is defined as a limit of the function  $H_m : [0, 1] \rightarrow [0, 1]^d$ , and these  $H_m$  are our main focus. We will now define these curves, loosely following the terminology from [11]. Firstly, for a given integer  $L$ , we consider a partition of the unit interval into  $2^L$  disjoint intervals: the semi-closed intervals  $I_L(\ell) = [\ell 2^{-L}, (\ell + 1) 2^{-L}]$  for  $\ell = 0, \dots, 2^L - 2$ , and the closed interval  $I(2^L - 1) = [(2^L - 1) 2^{-L}, 1]$ . We denote the collection of all these intervals by  $\mathcal{I}_L$ . For a natural  $d > 1$ , we also consider the partition of the unit hypercube  $[0, 1]^d$  into  $2^{L \cdot d}$  disjoint hypercubes of the form  $E_L^d(\vec{\ell}) = I(\ell_1) \times \dots \times I(\ell_d)$ . We denote the collection of these hypercubes by  $\mathcal{E}_L^d$ .

Next, for any given  $m$ , we define  $H_m$  to be a bijection from  $\mathcal{I}_{d \cdot m}$  to  $\mathcal{E}_m^d$ , such that (i) adjacent intervals are mapped to adjacent hypercubes and (ii) if  $I_{d \cdot (m+1)}(k') \subseteq I_{d \cdot m}(k)$  then  $H_{m+1}(I_{d \cdot (m+1)}(k')) \subseteq H_m(I_{d \cdot m}(k))$ . An illustration of  $H_m$ ,  $m = 1, 2, 3$  for  $d = 2$  is given in Figure 2. Each  $H_m$  maps a finite collection of intervals bijectively to a finite collection of hypercubes. This naturally induces a bijection from the grid defined by the intervals centroids, to the grid defined by the hypercube centroids. We denote these grids by  $\mathbb{A}[d \cdot m] \subseteq [0, 1]$  and  $\mathbb{B}[d, m] \subseteq \mathbb{R}^d$ , respectively.

The Hilbert curve  $H$  is obtained from  $H_m$  by a limiting procedure and shown to be Holder continuous [11]. Following similar ideas we show that each Holder function  $H_m$  is Holder continuous with constant that do not depend on  $m$ . This property will be crucial for the analysis of the covering number of the Hilbert canonization.

**Lemma A.5.** For every natural  $m, d$ , we have that

$$\forall x, y \in \mathbb{A}[d \cdot m], \quad \|H_m(x) - H_m(y)\|_\infty \leq 4|x - y|^{1/d}$$

*Proof.* Let  $x \neq y$  be points in the one dimensional grid  $\mathbb{A}[d \cdot m]$ , and assume without loss of generality that  $x < y$ . Note that  $y - x \geq \frac{1}{2^{d \cdot m}}$ , since this is the minimal distance between points in the grid. On the other hand,  $y - x \leq 1$ . Therefore, there exists some  $k$  with  $m - 1 \leq k \leq 0$ , such that

$$2^{-d \cdot (k+1)} \leq |x - y| \leq 2^{-d \cdot k}. \quad (6)$$

It follows that  $x$  and  $y$  are in two adjacent intervals in the  $k$ -th level (or in the same interval), and by the nesting property of Hilbert's curve, we know that  $H_m(x)$  and  $H_m(y)$  are in two adjacent hypercubes (or in the same hypercube). Therefore, their distances is at most the sum of the diameters of those two cubes, so

$$\|H_m(x) - H_m(y)\|_\infty \leq 2 \cdot 2^{-k} \stackrel{(6)}{\leq} 4|x - y|^{1/d}$$

□

**Hilbert Canonization** As a first step, we define a canonization not on all of  $[0, 1]^{d \times n}$ , but rather on the finite set of  $n$  tuples of grid elements  $\mathbb{B}^n[d, m]$ . This is done by mapping each tuple-element to the unit interval using  $H_m^{-1}$ , then sorting the resulting  $n$ -dimensional array, and mapping back to the  $d$ -dimensional grid using  $H_m$ . We denote this canonization by  $c_m$ . We can write  $c_m = H_m \circ \text{sort} \circ H_m^{-1}$ , with the understanding that  $H_m$  and  $H_m^{-1}$  are applied elementwise to  $n$ -tuples of grid elements.

To extend  $H_m$  to all of  $K = [0, 1]^{d \times n}$ , we employ the following procedure: For a given  $X = (x_1, \dots, x_n) \in K$ , (i) **Rounding:** Each  $x_j$  resides in a unique hypercube in  $\mathcal{E}_m^d$ . Replace  $x_j$  with the centroid of this cube  $y_j \in \mathbb{B}^n[d, m]$ . (ii) **Sorting:** find the permutation  $\tau \in S_n$  which sorts  $(H_m^{-1}(y_1), \dots, H_m^{-1}(y_n))$  from small to large. (iii) **Canonizing** Apply the permutation  $\tau$  to  $X$ . We note that if  $X$  contains several points in the same hypercube, the permutation  $\tau$  is not uniquely defined. In this case, the order of points with the hypercube will be determined by lexicographical sorting.

We now restate and prove our theorem regarding the covering number of the Hilbert canonization:

**Theorem 4.3.** Let  $d, n, m \geq 2$  be natural numbers, let  $\epsilon \in (0, 1)$ , and assume that  $\epsilon > 2^{-m-1}$ . Set  $K = [0, 1]^{d \times n}$  and  $\mathbb{G} = S_n$ . Then the covering number of the Hilbert canonization  $c_m$  satisfies

$$\mathcal{N}(c_m(K), \rho_\infty, \epsilon) \leq \binom{n + \lceil 1/(2\delta) \rceil - 1}{n}, \text{ where } \delta = \frac{(\epsilon - 2^{-m-1})^d}{4}$$

*Proof.* We first begin by a reduction from covering  $K$  to covering the grid  $\mathbb{B}^n[d, m]$ . For convenience we abbreviate  $\mathbb{B}^n := \mathbb{B}^n[d, m]$ . We note that for any  $X \in K$ , the matrix  $Y$  obtained by the rounding procedure satisfies  $\|X - Y\|_\infty \leq 2^{-m-1}$ . This stays true also after applying the canonization,  $\|c_m(X) - c_m(Y)\|_\infty \leq 2^{-m-1}$ , since the canonization will apply the same permutation to both  $X$  and  $Y$ . It follows that

$$\mathcal{N}(c_m(K), \rho_\infty, \epsilon) \leq \mathcal{N}(c_m(\mathbb{B}^n), \rho_\infty, \epsilon - 2^{-m-1}).$$

It remains to bound the right-hand side:

$$\begin{aligned} \mathcal{N}(c_m(\mathbb{B}^n), \rho_\infty, \epsilon - 2^{-m-1}) &= \mathcal{N}(H_m \circ \text{sort} \circ H_m^{-1}(\mathbb{B}^n), \rho_\infty, \epsilon - 2^{-m-1}) \\ &\stackrel{(*)}{\leq} \mathcal{N}(\text{sort} \circ H_m^{-1}(\mathbb{B}^n), \rho_\infty, \delta) \\ &\leq \mathcal{N}(\text{sort}([0, 1]^n), \rho_\infty, \delta) \\ &\stackrel{(**)}{\leq} \binom{n + \lceil 1/(2\delta) \rceil - 1}{n} \end{aligned}$$

Where  $(*)$  follows from the Holder properties of  $H_m$  proven in Lemma A.5, and  $(**)$  follows from the fact that one-dimensional sorting is an isometry (Proposition 3.3) and the upper bound on the covering number of  $[0, 1]^n/\mathbb{G}$  (Lemma 4.2). □

**Lemma A.6.** *Be  $K = [0, 1]^{n \times d}$  and  $\epsilon = \frac{1}{2^k} > 0$  such that  $k \in \mathbb{N}$ . Then  $\mathcal{N}(K, d_\infty, \epsilon) = \frac{1}{(2\epsilon)^{nd}}$*

*Proof.* It’s easy to see that each line we can cover using  $\frac{1}{2^k} \epsilon$  sized lines, so using the product of size covering for  $n \cdot d$  times we get a covering for  $K$  that uses  $\frac{1}{(2\epsilon)^{nd}}$  balls. On the other hand, denote by  $F$  some other covering. Note that  $K \subseteq \cup_{c \in F} B(c, \epsilon)$  So  $1 = \mu(K) \leq \mu(\cup_{c \in F} B(c, \epsilon)) \leq \sum_{c \in F} \mu(B(c, \epsilon)) = |F| \cdot (2\epsilon)^{n \cdot d}$  so  $\frac{1}{(2\epsilon)^{nd}} \leq |F|$ . Thus, we got the lower bound and the upper bound as desired.  $\square$

## B Additional Experiments

### B.1 Laplacian Eigenvector Sign Ambiguity: Augmentation vs. Canonization on ogbg-molpcba

This appendix presents an additional empirical comparison between deterministic canonization and training-time random group augmentation, on a setting distinct from the main-text experiments and complementary to the PCA experiment of Section 4. The goal is to ask whether the empirical behavior of these two strategies on a standard graph property prediction benchmark is qualitatively consistent with our Proposition 2.2 and the covering-number inequality (2); we do not claim a quantitative test of the inequality, since the test AP on a finite-sample-trained GIN mixes optimization, capacity, and generalization effects that the inequality does not isolate. The experiment is also consistent with the empirical observation cited in the Related Work that randomized SMILES can outperform canonized SMILES [1, 3].

**Module.** We study graph property prediction on ogbg-molpcba using a 5-layer Graph Isomorphism Network (GIN) with Laplacian positional encoding (LapPE). For each graph  $G$  with normalized Laplacian  $L_G$ , we compute the  $k$  smallest non-trivial eigenpairs  $\{(\lambda_i, v_i)\}_{i=1}^k$  and concatenate the eigenvectors as a node-level positional encoding. The resulting LapPE is invariant to graph isomorphism only up to the eigenvector *ambiguity group*

$$\mathbb{G}_{\text{LapPE}} = \prod_{i: m_i=1} \{-1, +1\} \times \prod_{i: m_i>1} O(m_i),$$

where  $m_i$  denotes the multiplicity of eigenvalue  $\lambda_i$ : a sign flip is admissible for each simple eigenvalue and an arbitrary orthogonal change of basis is admissible within each multiplicity- $m_i$  block. On molecular graphs, the spectrum is almost everywhere simple, so in practice  $\mathbb{G}_{\text{LapPE}}$  reduces to  $\{-1, +1\}^k$  for almost all graphs. The natural questions are then (i) whether to canonize this ambiguity, and (ii) whether augmentation-based approximations of group averaging behave consistently with our framework.

**Three methods compared.** We compare three strategies for resolving  $\mathbb{G}_{\text{LapPE}}$ , all implemented as faithful numpy ports of the reference torch code from the Laplacian canonization release of [20]. The first, `map` [20] (Maximal Axis Projection), resolves a simple-eigenvalue sign by forming the rank-one projector  $P_i = u_i u_i^\top$ , grouping the coordinate indices  $j$  by the rounded column norms  $\|P_i[:, j]\|$  (14-decimal rounding), and walking these groups from smallest to largest norm to find the first group whose indicator vector  $X$  (the sum of standard basis vectors over the group, plus a uniform shift) gives  $\|P_i X\| \neq 0$ ; the canonical sign is then  $\text{sign}(u_i^\top X)$ . For a multiplicity- $m_i$  block, `map` forms  $P = U_i U_i^\top$ , selects the  $m_i$  largest-norm coordinate groups, and builds the canonical orthonormal basis incrementally by projecting each group-indicator vector onto the residual orthogonal complement (with plain QR inside the complementary-space step). The second, `oap` [19] (Orthogonalized Axis Projection), differs from `map` in two places: the sign step rounds the column norms to 6 decimals (coarser tie-grouping under near-degenerate norms), and the basis step replaces the largest-norm groupings of `map` by a hash-based grouping of columns and uses signed-QR in the complementary-space iteration. The third, `random_augmented`, flips the sign of each eigenvector with probability  $1/2$  at every training-time forward pass, so the network sees a uniformly random element of  $\{-1, +1\}^k$  at each step. This is a finite-group augmentation that approximates group averaging over  $\mathbb{G}_{\text{LapPE}}$  without summing over its  $2^k$  elements explicitly. At evaluation time the `random_augmented` model is fed the deterministic eigsh-sign convention from the cache (no fresh

random draws), yielding a single deterministic prediction per graph; this is the number reported in the `random_augmented` column of Table 5. Note that this is an *adversarial* test-time deployment of an averaging-trained model (it scores a single point of the orbit rather than the orbit mean); the `AUG- $K$`  column reports the alternative Reynolds-style sample of  $K$  orbit elements, and we discuss the gap between the two below.

**Test-time averaging AUG- $K$ .** For `random_augmented` models we additionally evaluate a test-time *Reynolds-style* averaged metric. At evaluation, for each test graph we draw  $K$  independent group elements  $g_1, \dots, g_K \in \mathbb{G}_{\text{LapPE}}$  (each  $g_j$  a sign-flip pattern on the simple-eigenvalue subspace and a Haar-random orthogonal matrix on each multiplicity- $m$  block); we forward-pass the model on each sign-flipped LapPE; we average the predicted per-task probabilities; and we score the averaged predictions with the official OGB AP evaluator. We use  $K = 8$  at  $k = 3$  (which approximately covers  $\{-1, +1\}^3$  under uniform i.i.d. sampling: 8 draws cover  $\sim 65\%$  of the 8-element group on average) and  $K = 16$  at  $k \in \{8, 16\}$  (sparse Monte-Carlo over  $\{-1, +1\}^8$  and  $\{-1, +1\}^{16}$  respectively). On `ogbg-molpcba` the spectrum is almost everywhere simple, so the multiplicity-block factor  $\prod_i O(m_i)$  is degenerate in practice and the  $g_j$  samples reduce to sign-flip patterns. This is the empirical group-averaging operator of Section 2, restricted to a finite sample.

**Hyperparameters and protocol.** GIN, 5 layers, hidden dim  $h \in \{16, 128, 512\}$ , dropout 0.5, batch size 32, optimizer Adam with cosine learning-rate schedule and initial rate  $10^{-3}$ , 3 seeds per cell ( $\{0, 1, 2\}$ ), eigval-scaling off, eigenvector cache size 15. Checkpoint selection: the model state at the epoch with the highest validation AP across all training epochs is saved (ties broken by the earliest epoch); the final test AP reported in Tables 5 and 6 is this checkpoint’s score on the OGB test split. Software stack: PyTorch 2.10.0, CUDA 12.8, `torch_geometric` 2.7.0, `numpy` 2.2.6, `scipy` 1.15.3, `ogb` 1.3.6 (OGB evaluator: `Evaluator(name='ogbg-molpcba')`). Per-arm seeding via `torch.manual_seed`, `numpy.random.seed`, and `random.seed`; `cuda.deterministic` is not enforced, so two runs at the same seed on different hardware are not guaranteed to be bit-identical (we observe the resulting variability absorbed into the seed std at the magnitudes shown in Table 6). Standard deviations reported below are sample standard deviations (ddof = 1). Code, raw `results.json` files, the `orbit_stability.json` files behind Table 7, and reproduction commands are released at the project repository.

**Compute budget.** At  $k \in \{3, 8\}$  all three arms are trained for 200 epochs with early-stop patience 15. At  $k = 16$ , where validation AP for `random_augmented` continues to improve well past 200 epochs, all three arms are trained for 500 epochs with early stopping disabled (patience 999). Tables 5 and 6 therefore report a matched-compute comparison at every  $(k, h)$  cell. Both schedules are released in the project repository.

**Results.** Table 5 reports mean test AP at all nine  $(k, h)$  cells for the three methods, alongside the AUG- $K$  test-time-averaged metric for `random_augmented`. Table 6 zooms in on the  $k = 16$  slice with sample standard deviations.

**Test-time averaging  $\Delta$  is small.** Across all nine  $(k, h)$  cells the difference between the single-pass deterministic-eigsh evaluation of the `random_augmented` model and its AUG- $K$  averaged evaluation (Table 5, right-most two columns) lies in  $[-0.0002, +0.0005]$  AP, within the seed noise at every cell. The AUG- $K$   $\Delta$  is an aggregate metric, not a direct measurement of model invariance; we test invariance directly in the next paragraph.

**Per-graph orbit stability.** For each test graph we draw  $K = 64$  i.i.d. elements  $g_j$  of the sign-flip subgroup of  $\mathbb{G}_{\text{LapPE}}$ , forward-pass the trained `random_augmented` model on each  $g_j$  (LapPE), and record the per-task predicted probability. The resulting per-graph spread (max – min predicted probability across the  $K = 64$  draws) is a direct measure of how much the model’s output varies across orbit elements. Aggregating across all 43,793 `ogbg-molpcba` test graphs and 128 tasks, at hidden dim  $h = 128$  and over all 3 training seeds we observe a clean monotone scaling of per-graph spread with  $k$  (Table 7): mean per-graph spread is  $0.0013 \pm 0.0005$  at  $k = 3$ ,  $0.0027 \pm 0.0012$  at  $k = 8$ , and  $0.0048 \pm 0.0008$  at  $k = 16$ . This is qualitatively consistent with  $|\mathbb{G}_{\text{LapPE}}| = 2^k$ : more orbit elements give more room to vary, and the model is closer to be invariant for smaller  $k$ . The within-seed standard deviation of the OGB AP across the  $K = 64$  orbit elements is at most 0.0006 at  $k = 16$  and below 0.0004 at  $k \in \{3, 8\}$ , in every case much smaller than the between-seed standard

Table 5: Mean test AP on ogbg-molpcba at matched compute, 3 seeds per cell ( $k \in \{3, 8\}$  at 200 epochs / patience 15,  $k = 16$  at 500 epochs / patience 999 for all three arms). Per-cell row-best margins are mostly within seed std and none survives a Bonferroni correction across the nine cells at  $\alpha = 0.05$  (see Table 6 for the  $k = 16$  Welch  $p$ -values); the bolding, therefore, marks the nominal row-best mean, not a significance claim. The AUG- $K$  column reports test-time averaging over  $K$  ambiguity-group draws applied to the random\_augmented-trained model (see text).

$k$	$h$	map $\uparrow$	oap $\uparrow$	random_augmented $\uparrow$	AUG- $K$
3	16	0.0626	0.0641	<b>0.0662</b>	0.0663 ( $K = 8$ )
3	128	0.1704	0.1682	<b>0.1762</b>	0.1765 ( $K = 8$ )
3	512	0.2397	<b>0.2431</b>	0.2395	0.2398 ( $K = 8$ )
8	16	0.0622	0.0605	<b>0.0636</b>	0.0637 ( $K = 16$ )
8	128	0.1705	0.1754	<b>0.1766</b>	0.1766 ( $K = 16$ )
8	512	0.2344	0.2371	<b>0.2395</b>	0.2400 ( $K = 16$ )
16	16	<b>0.0716</b>	0.0703	0.0691	0.0693 ( $K = 16$ )
16	128	<b>0.1923</b>	0.1836	0.1916	0.1921 ( $K = 16$ )
16	512	0.2468	0.2419	<b>0.2483</b>	0.2481 ( $K = 16$ )

Table 6: Matched-compute  $k = 16$  slice of Table 5: all three arms trained for 500 epochs with patience 999. Reported are mean  $\pm$  sample standard deviation over 3 seeds, plus the two-sided Welch  $t$ -test  $p$ -value for the row-best mean against the row-second-best mean. None of the three row-best margins reaches  $p < 0.05$ , and after a Bonferroni correction across the nine cells in Table 5 ( $\alpha = 0.05/9 \approx 0.0056$ ) none of the row-best margins anywhere in the appendix is significant.

$h$	map	oap	random_augmented	Welch $p$ (best vs. 2nd)
16	<b>0.0716 <math>\pm</math> 0.0067</b>	0.0703 $\pm$ 0.0070	0.0691 $\pm$ 0.0008	$\approx 0.83$
128	<b>0.1923 <math>\pm</math> 0.0005</b>	0.1836 $\pm$ 0.0025	0.1916 $\pm$ 0.0009	$\approx 0.32$
512	0.2468 $\pm$ 0.0021	0.2419 $\pm$ 0.0028	<b>0.2483 <math>\pm</math> 0.0026</b>	$\approx 0.48$

deviation of the same quantity (0.0062 at  $k \in \{3, 8\}$ , 0.0015 at  $k = 16$ ): the model’s output varies less when we resample the ambiguity group at fixed seed than when we change the training seed at fixed ambiguity element. The Reynolds-style (mean-probability) AP across the  $K = 64$  draws is  $0.1923 \pm 0.0017$  at  $k = 16/h = 128$ , within seed noise of the matched-compute single-pass number ( $0.1916 \pm 0.0009$  for random\_augmented and  $0.1923 \pm 0.0005$  for matched-compute map at the same cell). We read this as direct evidence that the random\_augmented model is approximately  $\mathbb{G}_{\text{LapPE}}$ -invariant on the test distribution at the configurations tested, with the residual non-invariance growing predictably with the size of the ambiguity group. Along the hidden-dim axis at  $k = 16$  (Table 7, lower block, 3 seeds per cell), the per-graph spread is non-monotone in  $h$ :  $0.0032 \pm 0.0015$  at  $h = 16$ ,  $0.0048 \pm 0.0008$  at  $h = 128$ ,  $0.0033 \pm 0.0004$  at  $h = 512$ . We attribute this to a capacity floor and a capacity ceiling: at  $h = 16$  the network underfits (test AP  $\approx 0.07$ , near a constant-prediction baseline) so per-graph predictions are bunched near a few values and have little room to spread; at  $h = 512$  the network has enough capacity to learn invariance well; the middle case  $h = 128$  shows the largest residual non-invariance, although the  $h = 16$  row’s larger seed std (0.0015) suggests this conclusion is sensitive to which random initialization one looks at.

**Reading the tables.** Reading along the hidden-dim axis at fixed  $k$  in Table 5, the row-best AP grows monotonically with  $h$  at every  $k$ , and the row-best arm is most often random\_augmented (six of nine cells), with map nominally row-best at  $k = 16/h \in \{16, 128\}$  and oap nominally row-best at  $k = 3/h = 512$ . The matched-compute  $k = 16$  slice in Table 6 resolves these margins against seed variance: the smallest sample std on each row is consistently the random\_augmented std (0.0008, 0.0009, 0.0026), while map carries the largest std at small  $h$  (0.0067 at  $h = 16$ ). Under a two-sided Welch  $t$ -test for unequal variances, the row-best versus row-second-best margins at  $k = 16$  have  $p$ -values of 0.83, 0.32, and 0.48 at  $h = 16, 128, 512$  respectively, none significant. At  $k \in \{3, 8\}$  the row-best margins are similar in magnitude or smaller, with random\_augmented winning five of six rows there but at margins of the same order as the seed std. We therefore present Table 5 as a nominal-rank summary, not as a benchmark claim.

Table 7: Per-graph orbit stability of the trained random\_augmented model under  $K = 64$  uniform i.i.d. draws from the sign-flip subgroup of  $\mathbb{G}_{\text{LapPE}}$ , evaluated on the ogbg-molpcba test set (43,793 graphs  $\times$  128 tasks). All entries are the mean  $\pm$  sample standard deviation over the 3 training seeds. ‘‘Per-graph spread’’ is the mean over graphs and tasks of  $(\max - \min)$  predicted probability across the  $K = 64$  orbit elements. ‘‘Within-seed AP std’’ is the standard deviation of the OGB AP scored on each single orbit draw, averaged across seeds. ‘‘Reynolds AP’’ scores the mean probability over the  $K = 64$  draws. Per-graph spread scales monotonically with  $|\mathbb{G}_{\text{LapPE}}| = 2^k$ .

$k$	$h$	per-graph spread	within-seed AP std	Reynolds AP
<i>k axis at <math>h = 128</math> (3 seeds, <math> \mathbb{G}_{\text{LapPE}}  = 2^k</math>):</i>				
3	128	$0.0013 \pm 0.0005$	$\leq 0.0004$	$0.1764 \pm 0.0062$
8	128	$0.0027 \pm 0.0012$	$\leq 0.0005$	$0.1766 \pm 0.0062$
16	128	$0.0048 \pm 0.0008$	$\leq 0.0006$	$0.1923 \pm 0.0017$
<i>h axis at <math>k = 16</math> (3 seeds):</i>				
16	16	$0.0032 \pm 0.0015$	$\leq 0.0003$	$0.0694 \pm 0.0010$
16	128	$0.0048 \pm 0.0008$	$\leq 0.0006$	$0.1923 \pm 0.0017$
16	512	$0.0033 \pm 0.0004$	$\leq 0.0004$	$0.2481 \pm 0.0023$

**Tie to the theory.** On ogbg-molpcba at matched compute, with 3 seeds per cell, we did not detect a statistically significant difference between training-time random sign-flip augmentation and projection-based deterministic canonization at any of the nine  $(k, h)$  cells; this is qualitatively consistent with (2) of Proposition 2.2, which suggests that augmentation can match canonization on tasks where the covering number of  $\mathbb{G}$  is small, but it is not a positive test of the inequality, since AP gaps of order  $10^{-3}$  are dominated by optimization and seed noise rather than by the input-space covering complexity, the inequality bounds. The AUG- $K$  column moves AP by at most  $+0.0005$  across the nine cells; this is consistent with the cached deterministic eigsh-sign PE already lying close to the orbit-mean the network was trained on, but is not itself a direct test of model invariance.

## B.2 Explicit values of Covering Numbers

In this appendix, we compute the covering number bounds from Section 4 for specific values of  $\epsilon, d, n$ . We give bounds on the covering number of the quotient space  $K/\mathbb{G}$  when  $K = [0, 1]^{d \times n}$  and  $\mathbb{G} = S_n$ , as well as the covering number of the image of  $K$  under the Hilbert canonization and the Lexsort canonization, and the covering number of the hypercube  $[0, 1]^{d \times n}$  which is known to be  $k^{nd}$  when  $\epsilon = 1/(2k)$  (see proof in A.6). We take characteristic values encountered in point cloud learning scenarios: point dimensions are  $d = 3$ , a very modest value of  $\epsilon = 1/6$ , and  $n$  varying between 250 and 2000. The results are shown in Table B.2

Table 8: Comparison of covering number bounds as a function of  $n$  between the quotient space, the Hilbert and Lexsort canonizations, and the hypercube

Covering number vs. $n$	$n = 250$	$n = 500$	$n = 750$	$n = 1000$	$n = 2000$
Quotient (upper bound)	$2.1 \times 10^{36}$	$7.4 \times 10^{43}$	$2.2 \times 10^{48}$	$3.5 \times 10^{51}$	$2.0 \times 10^{59}$
Hilbert (upper bound)	$5.3 \times 10^{193}$	$7.9 \times 10^{278}$	$5.0 \times 10^{336}$	$5.0 \times 10^{380}$	$4.4 \times 10^{494}$
Lexsort (lower bound)	$1.1 \times 10^{239}$	$4.0 \times 10^{477}$	$1.4 \times 10^{716}$	$5.2 \times 10^{954}$	$9.2 \times 10^{1908}$
Hypercube (exact)	$6.9 \times 10^{357}$	$4.8 \times 10^{715}$	$3.3 \times 10^{1073}$	$2.3 \times 10^{1431}$	$5.3 \times 10^{2862}$

We note that our bounds for the quotient space and Hilbert canonizations are upper bounds, while the Lexsort bound is a lower bound. Thus, the gap between the covering number of Lexsort and that of the other methods may be even larger than shown in the table. We also note that despite the conservative choice of  $\epsilon = 1/6$ , all covering numbers in the table are enormous. This picture may be over-pessimistic, as the ‘true data distribution’ will be supported on a ‘small’ set  $K \subseteq [0, 1]^{d \times n}$  of ‘realistic point clouds’. An experiment estimating the covering number (in fact, the coverage) on the Modelnet40 dataset was shown in Table 1.

## C Experimental Setup and Hyperparameter Details

### C.1 Experimental Setup for the covering number experiment

We applied the following preprocessing for *each* sample: we first sample 256 points, then we shift it to the positive axis, and then divide by the maximum axis along  $x, y, z$ , obtaining all entries to be positive and between 0 and 1. The metric we considered on the point cloud space is

$$\rho_{\mathbb{G}}(X, Y) = \frac{1}{n} \sum_{i=1}^n \|X_i - Y_i\|_2.$$

The same metric is used for the two canonizations, and its quotient  $\rho_{\mathbb{G}}$  is used for the quotient space.

### C.2 Experiment setup: ModelNet40 classification

Table 9: Test accuracy of the Global MLP under varying training set sizes. The performance gap between Hilbert and lexicographical sorting widens as data becomes scarcer, highlighting the regularizing effect of optimal canonization.

Training Samples	None $\uparrow$	Lexicographical $\uparrow$	Hilbert $\uparrow$
9840 (full)	0.433	0.700	<b>0.748</b>
4920	0.408	0.641	<b>0.714</b>
2460	0.343	0.573	<b>0.673</b>
1230	0.307	0.504	<b>0.601</b>

In the ModelNet40 classification tasks, we sampled from each input CAD model point cloud, which consists of 1024 points, and applied an initial batched affine normalization to  $[0, 1]^3$ . The data is then ordered using one of three strategies: no canonization (baseline), lexicographical sorting (i.e., sorting points sequentially by their  $x$ , then  $y$ , then  $z$  coordinates), or Hilbert curve sorting (using a space size of  $2^{12}$ ). Following ordering, the coordinates are projected into a higher-dimensional space using Random Fourier Features to capture high-frequency geometric details. The feature vector is then passed through a bottlenecked MLP consisting of residual blocks with dimensions  $[256, 128, 64]$ , yielding the final classification logits. The MLPs were trained for 100 epochs with a fixed batch size of 256, and were trained using AdamW.

To ensure a rigorous and fair comparison between the different ordering strategies, we conducted comprehensive grid sweeps to identify the optimal hyperparameters for the uncanonized baseline (`ply`), lexicographical sorting (`lex`), and Hilbert curve sorting (`hilbert`). The specific optimal hyperparameters extracted from our sweeps and utilized for the final evaluation are detailed in Table 10. The best hyperparameters for each model on ModelNet40 are used for training the models on ModelNet10.

Table 10: Optimal hyperparameters identified via grid search for each ordering strategy.

Method	Learning Rate	Dropout	Weight Decay	Fourier Scale	Label Smoothing	Bands
No canon.	$1.63 \times 10^{-3}$	0.3	0.05	1.0	0.1	2
Lexsort	$6.41 \times 10^{-4}$	0.1	0.05	0.1	0.2	3
Hilbert	$9.61 \times 10^{-4}$	0.3	0.01	0.1	0.2	3

**Robustness Across Seeds** To account for variance in weight initialization and optimization dynamics, we evaluated the final optimal configurations across 5 independent random seeds. The averaged test accuracy and standard deviations are reported in Table 11. The results demonstrate that the Hilbert curve canonization not only achieves the highest average accuracy but also exhibits the lowest variance across different initializations.

Table 11: Test accuracy across 5 independent random seeds using the optimal hyperparameters. Hilbert canonization yields both higher performance and greater stability.

Method	Average Accuracy $\uparrow$	Standard Deviation
No canon.	0.433	0.0249
Lexsort	0.700	0.01358
Hilbert	<b>0.748</b>	0.00944

### C.3 Experimental Setup: Modelnet 40 Data scarcity experiment

To simulate data scarcity, we subsample the ModelNet40 training set using strides of 1, 2, 4, and 8, resulting in training subsets of 9840, 4920, 2460, and 1230 samples, respectively. Results are shown in Table 9.

### C.4 Experimental Setup: PCA group averaging

We use a DeepSets architecture that is fully invariant to point order permutations but strictly non-invariant to the  $\{-1, 1\}^3$  sign flips. We intentionally employ a lightweight, low-capacity version of this architecture. A highly over-parameterized model might achieve higher absolute accuracies, potentially masking the generalization gaps we aim to observe; by constraining the network capacity, we ensure that any performance differences are strictly attributable to the chosen alignment strategy. Each input point cloud consists of 1024 points from the ModelNet40 dataset. We compare four approaches: (1) **Pure PCA**, which leaves the sign ambiguity unresolved (acting as a baseline or potentially *poor* canonization due to eigensolver discontinuities); (2) **Skewness**, a deterministic canonization mapping  $c : K \rightarrow K$  that resolves the ambiguity by orienting axes based on the third moment; (3) **Frame Averaging**, an explicitly  $\mathbb{G}$ -invariant model constructed by pooling the network’s predictions across all 8 elements of the group using log-sum-exp; and (4) **Random Frame**, which applies elements of  $\mathbb{G}$  as random data augmentation during training. All models are optimized using Adam for 1600 epochs and evaluated across 5 different random seeds.

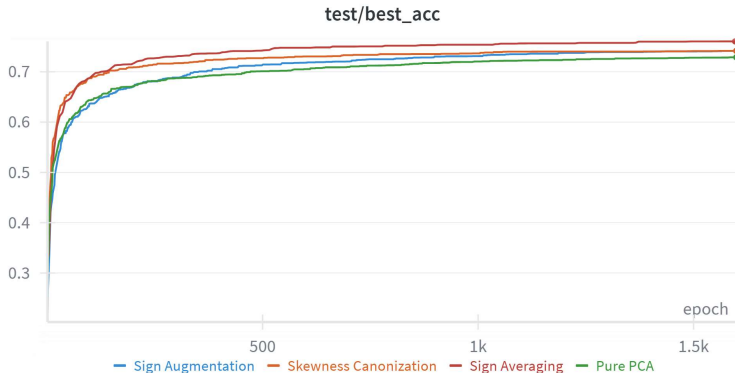


Figure 3: **Rotation Symmetry Accuracy.** The curves illustrate the comparative performance of the four approaches: Random Frame (blue), Frame Averaging (red), Skewness (orange), and the Pure PCA baseline (green). Frame Averaging achieves the strongest overall performance. While Random Frame and Skewness reach comparable final results—both significantly outperforming the Pure PCA baseline—the augmentation-based Random Frame method exhibits a noticeably slower convergence rate than deterministic canonization via Skewness.

### C.5 Experimental Setup: Rotated MNIST

In the last set of the experiments, we compare the performance of several image rotation invariant models. We considered three models: simple CNN, CN(p4)-CNN, and AvgCNN. The backbone for all three models is the same and additional layers are added for CN(p4)-CNN, AvgCNN. In order to have the same setting, including the data split we rerun all models, including CN(p4)-CNN. We used

learning rate of  $1e^{-3}$  and a batch size of 256 and an AdamW optimizer. Each experiment is run for 5 different seeds, and mean and standard deviation are reported.